Bulletin of the Geological Survey of Japan, vol. 43 (4), p. 207-235, 1992

Heat flow in the Izu-Ogasawara(Bonin) -Mariana Arc

Toshitsugu YAMAZAKI*

YAMAZAKI Toshitsugu (1992) Heat flow in the Izu-Ogasawara (Bonin) -Mariana Arc. *Bull. Geol. Surv. Japan,* vol. 43(4), p.207-235, 11 fig., 1 tab.

Abstract : This report presents 218 new heat flow data obtained from 1984 to 1989 in the Izu-Ogasawara (Bonin) -Mariana Arc. The purpose of the measurements is to evaluate the potential of hydrothermal activity and to understand better the tectonics of this region. Main target areas are (1) the Sumisu Rift, one of active backarc rifts in the northern Ogasawara Arc, (2) the Nishinoshima Trough, a paleorift of Oligocene (?) age in the middle Ogasawara Arc, which lies oblique to the strike of the present arc, and (3) the northern Mariana Trough from 20°N to 24°N.

The Sumisu Rift has high and variable heat flow values, which suggests the existence of hydrothermal circulation. Anomalously low temperature gradients (close to zero) are commonly observed in the upper several tens of centimeters of the surface sediments. Bioturbation by high activity of benthic organisms may be responsible for the low gradient. The Nishinoshima Trough is bounded on the west by a steep (max.1500m) fault scarp. Heat flow is generally higher in the trough than to the west of the scarp. This contrast would reflect difference in crustal thickness caused by old rifting. Local high heat flow associated with a intrusive body is observed in the trough. The Mariana Trough north of 22°N, which is now in a rifting stage, shows thermal asymmetry. High heat flow occurs only along the eastern margin of the trough. In the Mariana Trough south of 22°N, which has developed to a spreading stage, anomalous temperature profiles suggesting hydrothermal circulation are observed near the spreading centers.

1. Introduction

Extensive heat flow measurements were carried out in the Izu-Ogasawara (Bonin) -Mariana Arc as a part of the research program "Submarine Hydrothermal Activity in the Izu-Ogasawara Arc" from 1984 to 1989 using R/V Hakurei-maru. The purpose of the measurements is to know the thermal structure of these area and to obtain basic data to evaluate the potential of hydrothermal activity. This report presents 218 new heat flow data obtained through this research program, and briefly discuss their geological significance. Only a minor part of these data has been reported before (Yamazaki, 1988 ; Nishimura *et al.*, 1988).

The main target areas are (1) the Sumisu Rift, one of backarc rifts in the northern Izu-Ogasawara Arc, (2) around the Nishinoshima Trough and the Sofugan Tectonic Line, which is a geological structure obliquely crossing the middle Izu-Ogasawara Arc, and (3) the northern Mariana Trough (Figure 1). Geological settings and previous works of these areas are briefly introduced in the following.

In the northern Izu-Ogasawara Arc, topographic depressions, first noted by Mogi (1968), exist just behind the volcanic front (the Shichito Ridge) from Hachijojima Is. to Nishinoshima Is. These segmented depressions have been considered to be young (Karig and Moore, 1975) or Quaternary (Honza and Tamaki, 1985) extensional basins. These grabens are called the Hachijo, Aogashima, Sumisu, Torishima and Nishinoshima Rifts after nearby volcanic islands.

*Marine Geology Department

Keywords : heat flow, Izu-Ogasawara (Bonin) Arc, Mariana Trough, Sumisu Rift, backarc, rifting, hydrothermal circulation

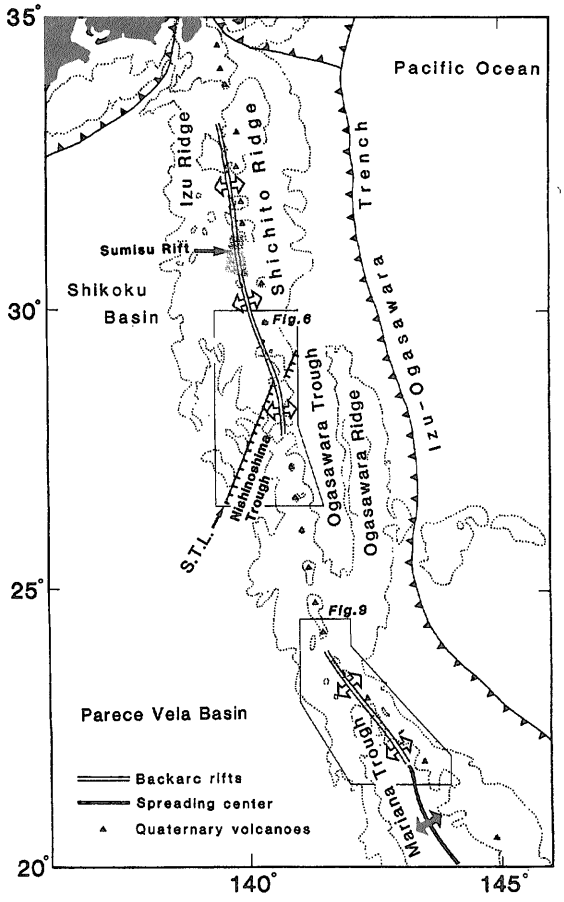

Fig. 1 Structural framework of the Izu-Ogasawara -Mariana arc. Dotted lines represent 1000m and 3000m iso-depths. S.T.L. : Sofugan Tectonic Line (modified from Yuasa (1985)).

Brown and Taylor (1988) and Murakami (1988) revealed detailed geological structure of the Sumisu Rift. Dives of submersible Alvin in 1987 discovered silica barite chimneys near the summits of dacite volcanoes in the Sumisu Rift (Taylor *et al.*, 1990 ; Urabe and Kusakabe, 1990). Recent ODP (Ocean Drilling Program) Drilling revealed that the floor of the Sumisu Rift is filled with volcaniclastic sediments not older than 1.1 Ma (Leg 126 Scientific Drilling Party, 1989).

In the backarc of the Izu-Ogasawara Arc, *en echlon* arrangement of topographic highs and lows oblique to the trend of the arc is remarkable (Karig and Moore, 1975 ; Honza and Tamaki, 1985). The most prominent among them is a steep cliff linearly trending SSW from south of Sofugan Island, which would probably be a normal fault. Yuasa (1985) considered that the Izu-Ogasawara Arc can be structurally divided into the southern and northern part by this fault, and called it the Sofugan Tectonic Line. The Nishinoshima Trough lies on the east of the Sofugan Tectonic Line. The Nishinoshima Trough is bordered on the east by the Shichito Ridge. (The "Nishinoshima Trough" of Honza and Tamaki (1985) and Yuasa (1985) includes other topographic lows lying between the Shichito Ridge and the Izu Ridge, but in this report does not). Yuasa (1991,1992) proposed that the Nishinoshima Trough was formed as a northern tip of the incipient opening of the Parece Vela Basin in Oligocene time (Mrozowski and Hayes, 1979). The sediment thickness on the acoustic basement of the Nishinoshima Trough exceeds 2 km in the southwestern part, and it decreases towards northeast.

A few workers reported heat flow data in the Izu-Ogasawara Arc (Vacquier *et al.*, 1966 ; Watanabe *et al.*, 1970 ; Matsubara, 1981). But, the amount of the data was still too small to discuss thermal structure and hydrothermal activity of the arc.

The Mariana Trough is known as one of active backarc basins on the globe (Karig, 1971). The rifting of the Mariana Trough is considered to have begun in the latest Miocene (Hussong and Uyeda *et al.*, 1982). Recent researches of the Mariana Trough including the DSDP drilling have been focused at the area of 18°N latitude (Anderson, 1975 ; Bibee *et al.*, 1980 ; Sager, 1980 ; Hussong and Uyeda *et al.*, 1982 ; Lonsdale and Hawkins, 1985). Extremely high heat flow values were observed there (Hobart *et al.*, 1983), and active hydrothermal vents were discovered by submersible Alvin (Craig *et al.*, 1987 ; Moore and Stakes, 1990). On the other hand, studies in other areas of the Mariana Trough have yet been scarce, and heat flow data were reported sparsely (Watanabe, 1970 ; Sclater *et al.*, 1972 ; Anderson, 1980 ; Yamano, 1985). Most of my measurements in the Mariana Trough are concentrated in the northern part from 20° to 24°N, and 67 new data in the area are presented in this report.

2. Data acquisition and reduction

2.1 Thermal gradient

I used four sets (three types) of temperature recorders. They are two GH80-1 type, a NTS10 type, and a NTS11 type recorders manufactured by Nichiyu-Giken Co. The GH80-1 type recorder has three channels for thermistors and 2 mK resolution (Matsubayashi, 1982). The NTS10 type has three channels, and the NTS11 has six. The resolution of both NTS10 and NTS11 type is 1 mK. The NTS11 type has a tilt sensor. Temperature data were digitized every 15 or 30 seconds except for sites from H111 to H138 at which they were every 60 seconds.

Several types of thermistor probe systems penetrating sediments were provided, and they were properly used depending on the stiffness of bottom sediments and on the purpose of measurements. They are (1) a 2m long gravity corer or a piston corer of 4 or 8m long with three to six thermistor probes mounted in outrigger fashion (Ewing type), (2) a 1.5 or 2.5 m long lance without coring which was equipped with three to six thermistor probes in outrigger fashion (Ewing type), (3) a thin (20 mm in diameter) probe of 0.7 or 0.9 m in length to which three to five thermistors were attached (Bullard type). A weight of about 500 kg were used for the systems of types (1) and (2), and that of about 50 kg for the type (3). The systems of types (2) and (3) allow multiple penetration during a single lowering. The type (3) system was used only in the Sumisu Rift.

Each thermistor was sealed in a teflon tube, and capped by a brass tube of 5 mm in diameter. The thermistor in each probe of the type (1) and (2) systems was at 2 to 3 cm from the outrigger fins. This distance might not be long enough to completely avoid effects of axial heat conduction, but I believe it did not cause serious error. Thermistor probes were angularly offset from each other so that no probes passes through the same sediments.

Decay of frictional heating of the thermistors during penetration into sediments was monitored for 10 to 15 minutes. Equilibrium temperature of each thermistor was obtained by the extrapolation

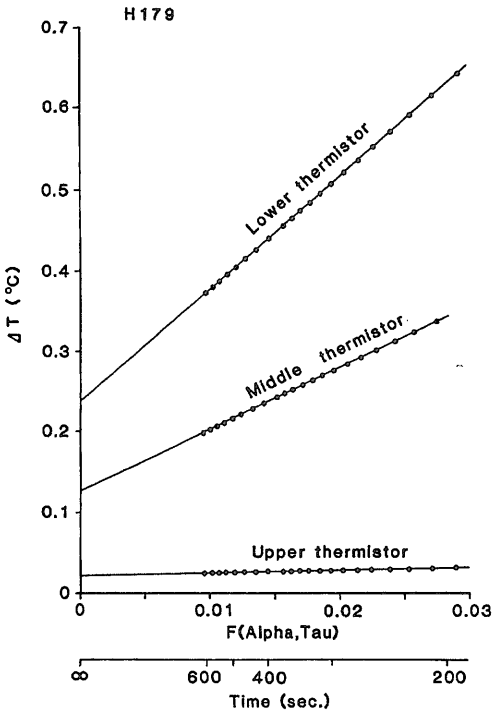

Fig. 2 Plot of thermistor temperatures versus $F(\alpha, \tau)$ of Bullard (1954) for frictional heating decay at site H179. Best-fit lines are calculated for each thermistor using the least squares method. The intercept at $F(\alpha, \tau)=0$ gives the equilibrium temperature.

using cylindrical decay function $F(\alpha, \tau)$ of Bullard (1954). A typical example is shown in Figure 2. I used a simple linear fit to the $F(\alpha, \tau)$ vs. temperature plot. The decy origin time was adjusted by trial and error to get linear $F(\alpha, \tau)$ decay (Villinger and Davis, 1987). Thermal disturbances due to the movement of the probe during the frictional decay monitoring cause nonlinear, anomalous $F(\alpha, \tau)$ decay plots, and these measurements were discarded.

2.2 Thermal conductivity

Thermal conductivity was measured on sediment cores by a QTM (Quick Thermal Conductivity Meter, Showa Denko Co.). This instrument adopts a transient line-heat-source method (Ito *et al.*, 1975). The QTM was calibrated using standards of fused quartz and acrylic resin (manufacture's recommended values are 1.39 and 0.241 W/mK, respectively). The accuracy is within ±

5% (Sass *et al.*, 1984 ; Galson *et al.*, 1987).

The sediment cores were split in halves and covered with thin plastic film (commercial transparent food-wrapping film) to prevent evaporation of pore water before measurement. The effect of this film on the conductivity is negligible (Sass *et al.*, 1984). Measurements were done on board as soon as the thermal steady state was attained at room temperature (20 to 25℃) a few hours after the core was retrieved. The values measured in the laboratory were corrected to *in situ* conditions of temperature and pressure following Ratcliffe (1960). For the sites where no sediments were obtained due to multiple-penetration measurements or failure of coring, the conductivity at the nearest site was adopted.

2.3 Positioning and shipboard operation

Real-time navigation of the ship was done by Loran-C, which was calibrated by satellite fixes (NNSS). Absolute accuracy of the ship's position is about 100m after post processing. A position of a heat flow probe relative to the ship could not be known accurately because we did not use an acoustic positioning system. But it would be almost just under the ship because during the measurements the ship was not let drifting but was controlled strictly to keep wire angle as vertical as possible. The amount of slack wire while the instrument was in the bottom was only 3 to 5m in usual.

Our procedure of the multi-penetration measurement was as follows. After one measurement, we raised the instrument up to 100m (sometimes 1000m) above the seafloor. We moved slowly (about 2 knots) to the next station which was several hundred meters apart, and then letting the wire angle as vertical as possible before the next penetration. We could make more than one measurement per hour.

The positions of the measurement sites listed in Table A-1 are based on the Tokyo geodetic datum except for the sites at the Mariana Trough 18°N (H334, H335, H336 and H338) which are based on the WGS-72. Note that the difference between the two system is as much as several hundred meters.

3. Results

The results of 218 successful heat flow measurements are summarized in Table A-1.

Temperature profiles in sediments are presented in Figure A-1. The accurate depths to which probes penetrated could not be known while rough estimation of them are included in Table A-1. Thus, the lengths of the probes are adopted as vertical axes in the figures. When bottom sediments were soft enough to be penetrated, lower part of core head in which the pressure vessel of the temperature recorder was placed was buried in the sediments. In this case the tip of the probe would have reached to the depth of 1 to 2m more than the length of the probe.

An error of a temperature of each thermistor is assigned as

$$\Delta T = \pm (0.005 + 0.001 \cdot G) \quad (°K)$$

where G is a gradient of the line being fitted on the $F(\alpha, \tau)$ vs. temperature plot of frictional heat decay $[dT/dF(\alpha, \tau)]$. The latter term is introduced because a larger error in the determination of equilibrium temperature may be expected for larger frictional heating on penetration into hard sediments. The estimated uncertainty of the extrapolated temperature at ordinary sites with moderate frictional heating is about ± 10 mK. At some sites of hard bottom sediments such as in the Sumisu Rift and a part of the Mariana Trough, it exceeds ± 20 mK. Temperature data of some sites are considered to be less reliable, and such sites are noted in Table A-1. The reasons are that small thermal disturbance was recognized on the frictional decay plots or the corer fell down before the completion of the frictional decay monitoring.

Thermal gradient was obtained in principle by fitting a straight line using the least-squares method when temperatures at three or more different depths were available. The gradients of some sites were calculated from only two temperature points. These data should be treated as low-grade ones, and are noticed in Table A-1.

Temperature profiles are significantly nonlinear at some sites. Several naturally occurring

phenomena can be responsible for a non-linear temperature profile (Noel, 1984). That is, vertical pore water advection, changes in bottom water temperature, sedimentation effects such as slumping and erosion, local topographic effect, *etc*. It is difficult, however, to specify the cause of these non-linearities unless closely spaced dense heat flow measurements and detailed data of local topography, sedimentation and bottom water temperature variation are available. For this reason, a straight line was fitted even in the case of the non-linear temperature profile, and these sites are noted in Table A-1. The sites in the Sumisu Rift are exceptions. Thermal gradients obtained from the two lowermost thermistors in the sediments were adopted, which will be discussed later.

No correction for sedimentation, surface and basement topography have been applied because this report puts emphasis on presenting data. However, effects of these factors are of course not negligible. They will amount up to 30% because many of the measurement stations would have fairly high sedimentation rate and rough topography.

Unfortunately, most of the penetrations in the Sumisu Rift reached to the depth of only 1m or less, and many heat flow values were calculated from the temperatures of only two thermistors. A well-sorted volcanic ash layer is encountered within 1m below the seafloor in the whole South Basin of the Sumisu Rift (Nishimura and Murakami, 1988). This ash layer causes large friction against the penetration of the probes. The Ewing probe using a gravity corer of 2m long often fell down on the hit to the bottom. Even in the case of successful penetration, extremely large frictional heat caused a large error in extrapolating equilibrium temperature. If we abandon to penetrate the ash layer, measurements in soft hemipelagic mud of less than 1m thick on the ash layer can be done easily using the thin Bullard probe of light weight.

4. Discussion

4.1 The Sumisu Rift

Heat flow values of 40 measurements in the Sumisu Rift range from 0 to 700 mW/m^2. These values have large uncertainty because the quality of the data there is low as mentioned above. However, we can safely say that both high and low values exist in a narrow area (the detailed survey area) (Figure 3). The existence of high values and local variability can be explained by hydrothermal circulation. Conductive effects (e.g. the effects of surface topography and basement topography) cannot explain such local variability.

At the ODP drilling sites in the Sumisu Rift, chemical composition of pore water in the sediments is not different from that of sea water (Leg

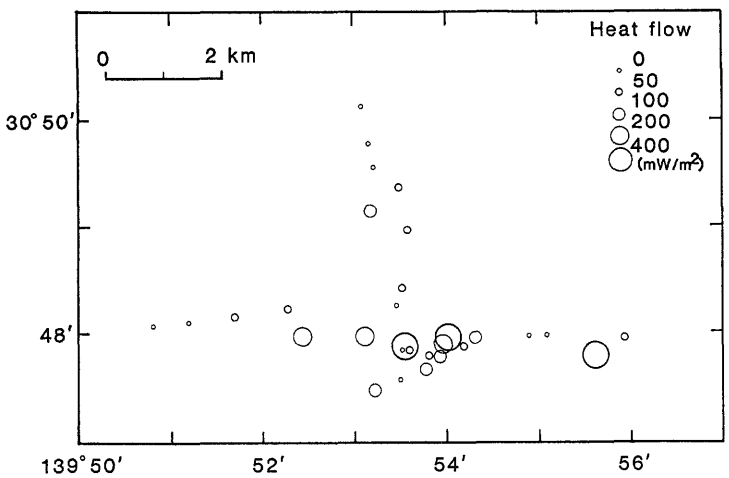

Fig. 3 Distribution of heat flow values in the detailed study area in the South Basin of the Sumisu Rift.

126 Scientific Drilling Party, 1989). This is probably because the ODP sites would be located in a recharge zone of hydrothermal circulation. Low heat flow values (less than 60 mW/m^2, H370-1, 2) are observed in the immediate vicinity of one of the two ODP sites (Site 791) (no data at another site).

Anomalously low temperature gradients (sometimes close to zero) are commonly observed in the surface sediments of several tens of centimeters in the detailed survey area of the Sumisu Rift (H322, H327, H331, H370, H371, H374, H379) (Figure A-1). The thin Bullard probe of light weight was used at all these sites. The gradient determined using the lowermost two (but less than 1m in depth) thermistors is considerably higher than that of the near-surface thermistor pair. Submersible Alvin made temperature measurements within the depth of 50 cm in the detailed survey area and found similar low gradient (K. Becker, personal communication, 1989).

It is difficult to specify the cause of the low gradient, but a possible explanation is well-mixing of cold bottom water with the surface sediments by intensive bioturbation. Observation by Alvin revealed that the activity of benthic organisms are very high on the floor of the Sumisu Rift (A. Nishimura, personal communication, 1989). Generally, non-linear, downward convex temperature profiles can be caused by variations of bottom water temperature or sudden deposition of surface sediments by turbidite. The latter seems unlikely in the Sumisu Rift judging from the lithology of the surface sediments, hemipelagic mud. The former mechanism cannot be excluded, but the possibility of the temperature variation of short periods such as the annual variation can be rejected because the data taken in different seasons and years have similar tendency. The temperature gradients of the deepest pair of thermistors are used here for the calculation of heat flow values because they are considered to be least disturbed no matter what is the cause of the low gradient.

It is rather confusing that the measurements using the heavy gravity corer show a tendency of having a higher thermal gradient than those by the small Bullard probe, and the former dose not show the surface low gradient. The example is H206 and H379-2 (Figure A-1). They are located at almost the same point, and the penetrated depths seem to be nearly equal to each other. The gravity corer was used for the former site and the Bullard probe for the latter. At H379-2, all five thermistors of 20 cm intervals penetrated the sediments, and only the deepest pair showed large gradient. At H206, on the other hand, two thermistors of 45 cm interval in the sediments showed larger gradient than the deepest part of H379-2. The uppermost thermistor of H206 has no sign of having penetrated the sediments. A possible explanation for this discrepancy is disturbance of the sediments by the gravity corer as illustrated in Figure 4. The surface hemipelagic mud may be scattered by the hit of the thick, heavy gravity corer of high penetrating speed, which will cause the apparent loss of the surface low gradient. Furthermore, the depth of the gradient measurement may be larger in actual at H206 using the gravity corer than at H379-2 using the Bullard probe. Downwarping of the hard ash layer by the large friction during the penetration of the gravity corer would cause the increase in temperature gradient. On the other hand, the sediments would be less deformed by slowly lowered thin Bullard probe of light weight. In the Sumisu Rift thus the measurements by the gravity corer may have overestimated the temperature gradient.

4.2 Around the Nishinoshima Trough

The distribution of heat flow values in the middle Ogasawara Arc from Sofugan Is. to Nishinoshima Is. is shown in Figure 5. The area east of the Sofugan Tectonic Line has generally higher heat flow than the area west of it. The Nishinoshima Trough has relatively uniform heat flow of about 100 mW/m^2 except for some sites which will be mentioned later. Co-existence of high and low heat flow values is observed in small grabens along the Shichito Ridge, which suggests the existence of hydrothermal circulation. These grabens are considered to be incipient rifts like the Sumisu Rift although their size is much smaller. The area west of the Sofugan Tectonic Line, on the other hand, has generally low heat flow. The Sofugan Tectonic Line is considered to be a large normal fault system which bounds the west-

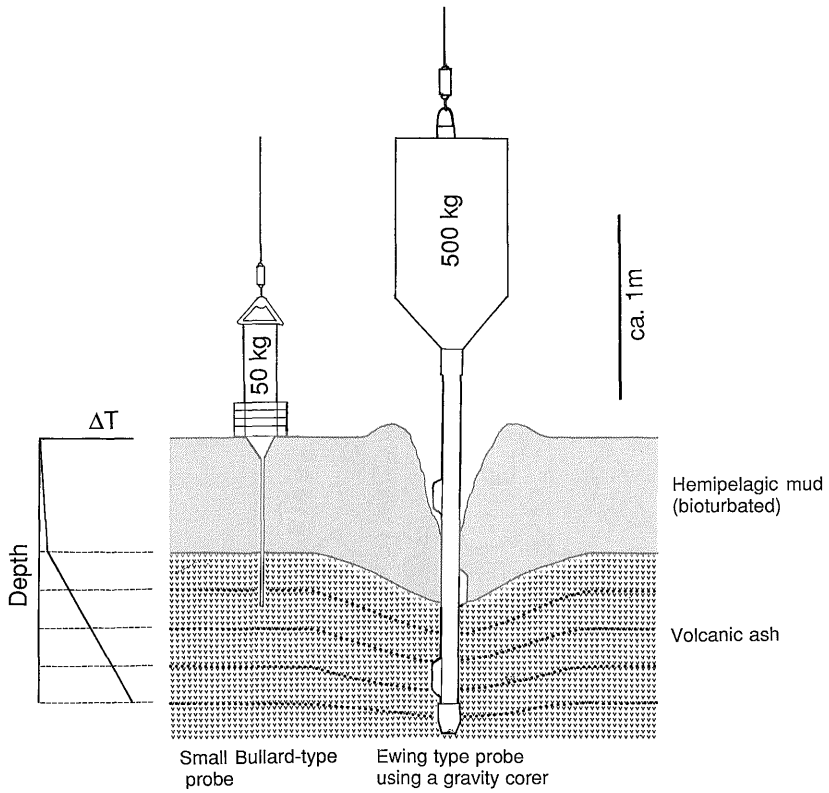

Fig. 4 A schematic diagram of the measurement in the Sumisu Rift. Temperature gradient of the surface sediments of several tens of centimeters (highly bioturbated hemipelagic mud) is very low. Well-sorted volcanic ash layer underlying the hemipelagic mud is hard to be penetrated. The penetration using a gravity corer may seriously disturb the sediments, which can cause overestimation of the gradient.

ern end of the rift graben of possibly Oligocene age. The contrast in heat flow would reflect the difference in crustal thickness caused by the past rifting.

Extremely high heat flow values over 400 mW/m^2 (H168 and H200-3) are observed in the southwestern part of the Nishinoshima Trough (26°52.0'N, 139°46.0'E) (Figure 5). An intrusive body exists in the thick sediments just blow the high heat flow sites, which is clearly shown on a seismic reflection profile (Figure 6). Disturbance of the very surface sediments probably caused by the intrusion can be recognized on a 3.5 kHz echogram (Figure 6). The high heat flow and the recent deformation of the sediments indicate that the intrusive activity is quite young. Multi-penetration measurements revealed the existence of a low heat flow site (45 mW/m^2, H200-4) close to the high heat flow sites (Figure 7), suggesting the occurrence of local hydrothermal circulation. Several similar intrusive bodies are found on seismic reflection records in the trough.

Two sites on or close to the Sofugan Tectonic Line (H171 and H173) show high and low values, 217 and 65 mW/m^2, respectively. Pore water circulation through this fault system would be responsible for the variation of heat flow values.

To the northwest of the Nishinoshima Trough, another SSW trending depression lies parallel with it (from 29°N, 139°59'E to 28°N, 139°20'E) (Figure 5). The strike of the depression suggests that its origin is related to the past rifting which formed the Nishinoshima Trough although the relief of the basement of this depression (max. several hundred meters) is much smaller than

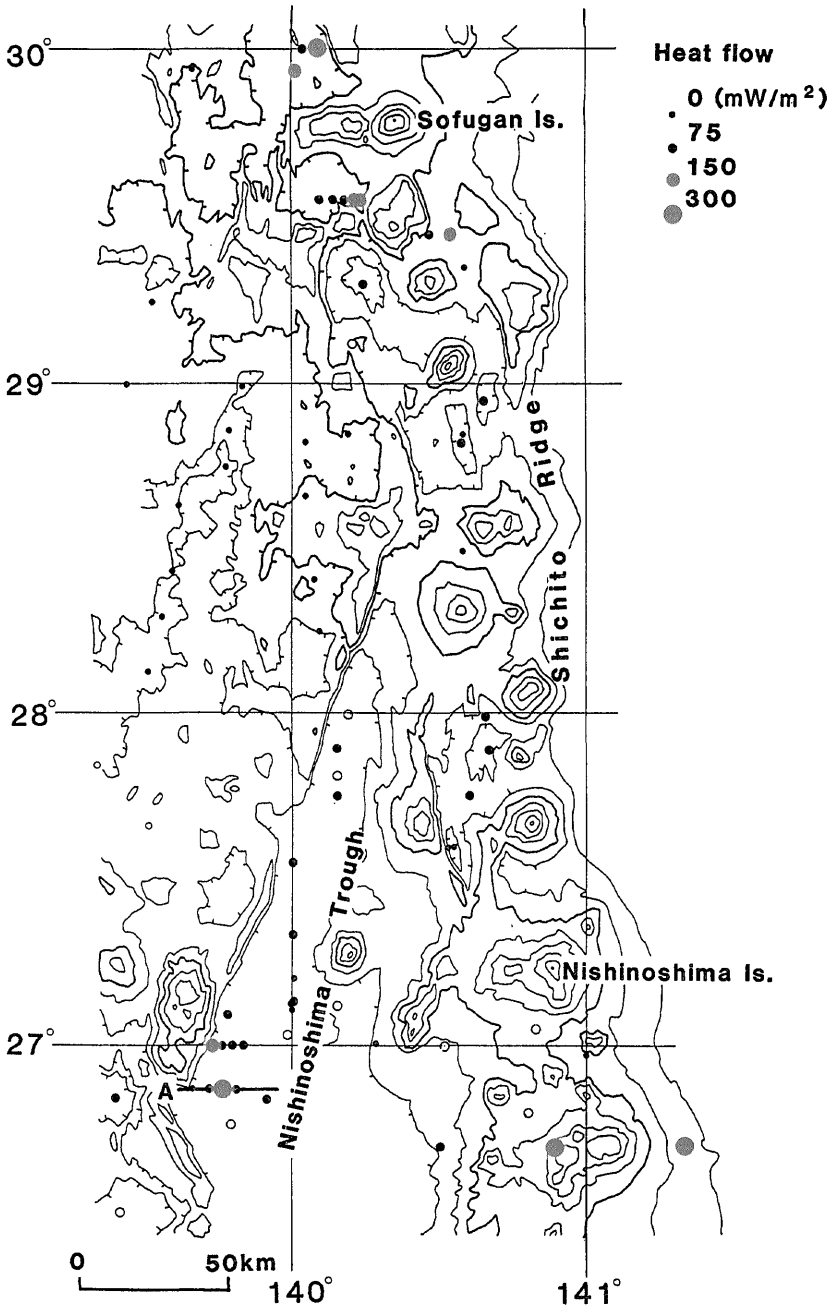

Fig. 5 Distribution of heat flow values in the Nishinoshima Trough and its environs. Solid circles are the data of this study, and open circles are from Vacquier *et al.* (1966), Anderson (1980) and Yasui (unpublished). Topographic contours are at 500m intervals. Bold contours are 2500m iso-depths. Line A is the location of the seismic profiles shown in Figure 6.

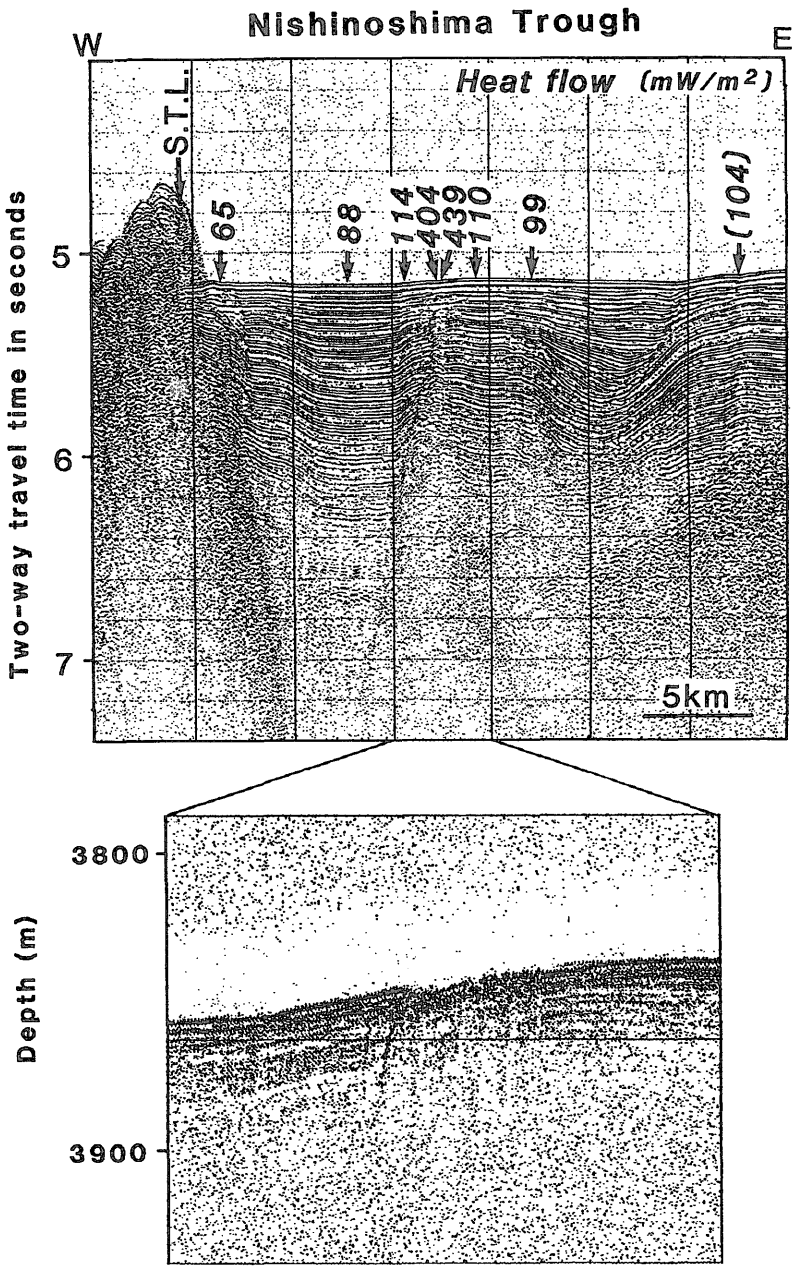

Fig. 6 A single-channel airgun seismic profile (top) and a 3.5 kHz echogram (bottom) running through a high heat flow point in the Nishinoshima Trough. The location of this line is shown in Figure 5. High heat flow values occur just above a intrusive body. The heat flow value in the parentheses was measured not on this line but at about 2 miles south. S.T.L. : the Sofugan Tectonic Line of Yuasa (1985).

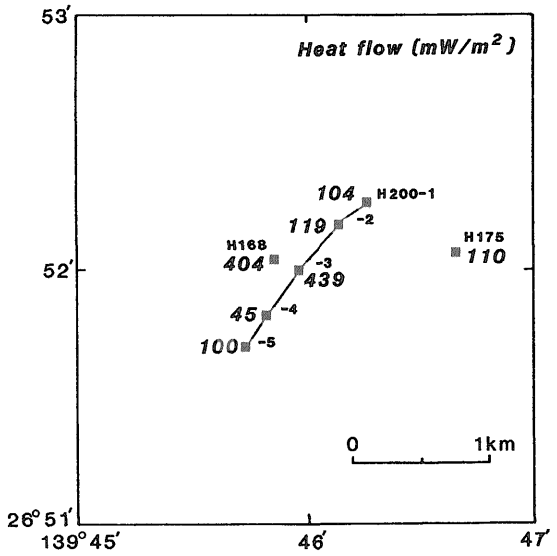

Fig. 7 Detailed heat flow measurements around the high heat flow point in the Nishinoshima Trough.

that of the Nishinoshima Trough. Eleven measurements in this depression showed uniformly very low heat flow, less than 30 mW/m^2 (from H139 to H145, H291), which is in contrast with the moderate or high heat flow in the Nishinoshima Trough. This value is too low for the conductive component of the heat flow from the oceanic island-arc of not older than Eocene age. It is thus considered that some heat should be transported by convection. Although the depression is well sedimented (about 300 m in thickness) and no outcrops of basement occur within 5 km of the measuring sites, long wave-length (10 km or more ?) pore-water advection may have occurred here.

4.3 The northern Mariana Trough

The Mariana Trough north of 22°N is considered to be now in a rifting stage based on geological structure and magnetic anomalies (Yamazaki *et al.*, 1988, 1991 ; Murakami *et al.*, 1989). The rifting north of 22°N is characterized by thermal and structural asymmetry. High and variable heat flow are observed only in or close to a row of small grabens along the eastern margin of the trough (Figure 8). The floor of the rift is comprised of tilted blocks bounded by normal faults, and steps down to the east (Figure 9). Except for the eastern margin, the trough has uniformly low heat flow. In the trough north of 22°N, therefore, the existence of hydrothermal activity can be expected only along the eastern margin.

Patterns of heat flow across rifts can give significant constraint on the mode of lithospheric extension during rifting (Buck *et al.*, 1988 ; Martinez and Cochran, 1989). The discovery of the thermal asymmetry of the northern Mariana Trough is hence important to understand better the rifting processes here. This subject is beyond the scope of this report, and will be discussed elsewhere (Yamazaki, 1992).

The Mariana Trough south of 22°N, on the other hand, has developed to a spreading stage (Yamazaki *et al.*, 1988, 1991 ; Murakami *et al.*, 1989). Spreading centers there can be identified from geological structure and magnetic lineations. Anomalous temperature profiles in sediments suggesting intense hydrothermal circulation are observed at several sites close to a spreading center.

Extraordinary large temperature difference between the uppermost thermistor in the sediments and bottom water is observed at H341 although the thermal gradient among three thermistors is low (Figure A-1). The depth of the penetration of the probe could not be known accurately, but

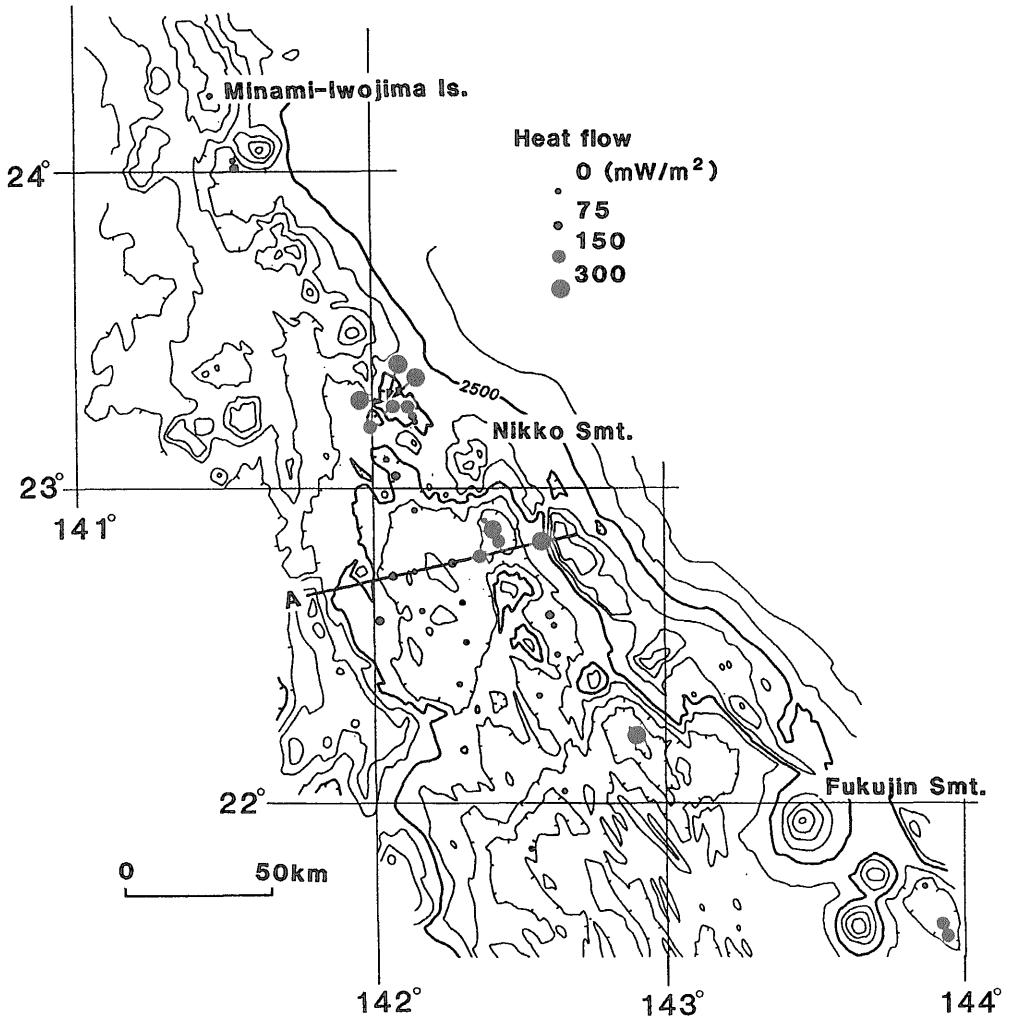

Fig. 8 Distribution of heat flow values in the northern Mariana Trough. High heat flow occurs only in or close to a row of small grabens along the eastern margin of the trough. Topographic contours are at 500m intervals. Bold contours are 2500m iso-depths. Line A is the location of the seismic profile shown in Figure 9.

the temperature profile of subsurface 1 or 2m at this site must be extremely non-linear. Furthermore, temperature gradients among sites around H341 are highly variable. H377-1 through H377-5 lie on a line starting from H341 at about 300m intervals (westward), and H342-1, -2 and -4 at 300 to 800m intervals (southward) (Figure 10). H377-1, which is located nearest to H341, and H377-5 show slightly upward convex subsurface temperature profiles. The rest are, on the other hand, linear and relatively low temperature gradients. The gradient of H342-4 is close to zero. These anomalous temperature profiles and local variations in the gradient can be explained by hydrothermal circulation. Pore water would be moving upward at H341, and nearby low-gradient sites would be in a recharge zone (Figure 10).

Another type of a shallow hydrocirculation effect can be seen at H344 and H367, showing temperature profiles with bends in the middle. The measurements were done independently (separate cruises), but the two sites are only ab-

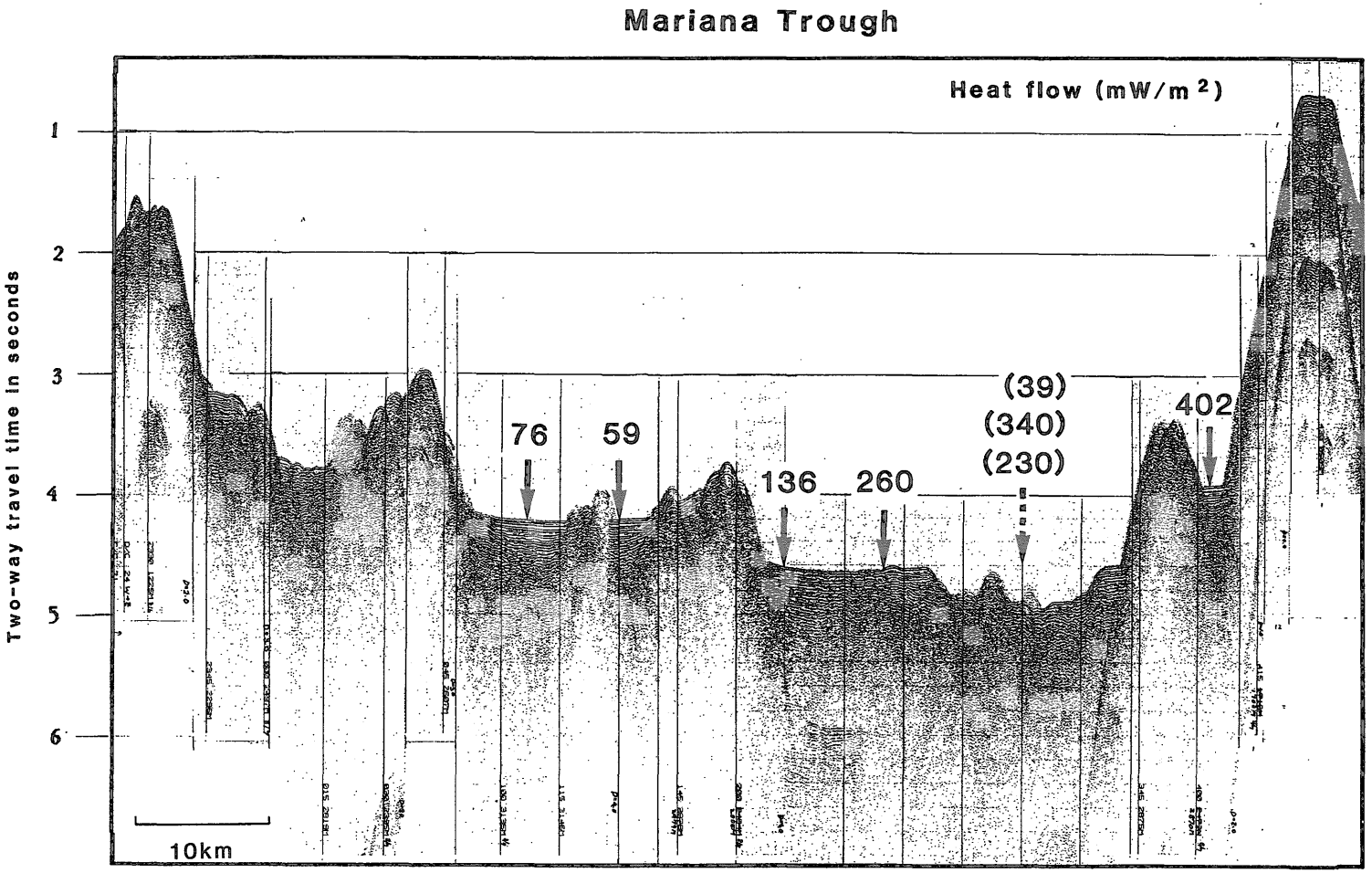

Fig. 9 A single-channel airgun seismic profile crossing the northern Mariana Trough at 23°N and heat flow values on this line. The location of the line is shown in Figure 8. The rifting at the northern Mariana Trough shows thermal and structural asymmetry. Heat flow values in the parentheses are located not on this line but in the northern continuity of the basin.

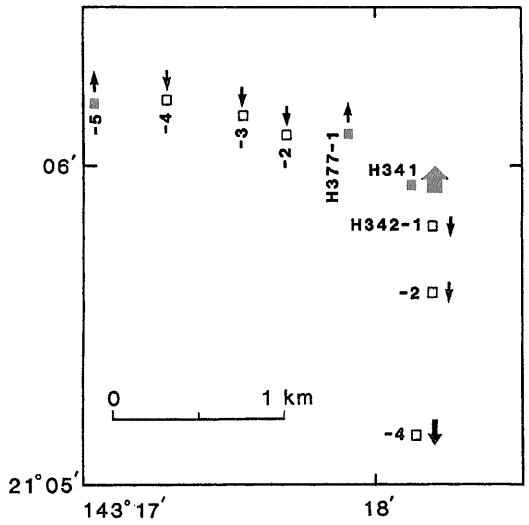

Fig. 10 Pore water circulation deduced from temperature profiles in sediments. This area is located close to the spreading center of the Mariana Trough at 21°N. The direction of the arrows (up or down) shows the direction of the pore water movement. The width of the arrows represent the relative intensity of the pore water movement. Solid squares are the sites at which non-linear temperature profiles (upward convex) are observed. Open squares are the sites of linear profiles.

out 300m apart. The two anomalous profiles are good evidence for lateral flow of pore water near the crest of an active spreading center.

Acknowledgements : The heat flow measurements were performed with cooperation of all on-board scientists, officers and crew of the Izu-Ogasawara-Mariana cruises of R/V Hakureimaru. I wish to thank A. Nishimura, F. Murakami, E. Saito, M. Yuasa and A. Usui for help and discussion through this work. I also thank K. Becker and B. Taylor for giving me unpublished data, M. Yamano for allowing me to use his compilation of heat flow data around Japan, and O. Matsubayashi for useful comments on the manuscript. This work was supported by the special research program, "Submarine Hydrothermal Activity in the Izu-Ogasawara Arc", funded by the Agency of Industrial Science and Technology from 1984 to 1989.

References

Anderson, R.N. (1975) Heat flow in the Mariana Trough. *J. Geophys. Res.*, vol. 80, p. 4043-4048.

——— (1980) 1980 update of heat flow in the east and southeast Asian sea. *In* Hayes, D.E. (ed.), *The tectonic and geologic evolution of southeast Asian seas and islands,* Geophysical Monograph, vol. 23, American Geophysical Union, Washington, D.C., p. 317-326.

Bibee, L.D., Shor Jr., G.G. and Lu, R.S. (1980) Inter-arc spreading in the Mariana Trough. *Mar. Geol.*, vol. 35, p. 183-197.

Brown, G. and Taylor, B. (1988) Sea-floor mapping of the Sumisu Rift, Izu-Ogasawara (Bonin) Island Arc. *Bull. Geol. Surv. Japan*, vol. 39, p. 23-38.

Buck, W.R., Martinez, F., Steckler, M.S. and Cochran, J.R. (1988) Thermal consequences of lithospheric extension : pure and simple. *Tectonics*, vol. 7, p. 213-234.

Bullard, E.C. (1954) The flow of heat through the floor of the Atlantic Ocean. *Proc. Roy. Soc. Lond. Ser. A*, vol. 222, p. 408-429.

Craig, H., Horibe, Y., Farley, K.A., Welhan, J.A., Kim, K.-P. and Hey, R.N.(1987) Hydrothermal vents in the Mariana Trough : results of the first Alvin dives. *EOS Trans.*, vol. 68, p. 1531.

Galson, D.A., Wilson, N.P., Schärli, U. and Rybach, L. (1987) A comparison of the divided-bar and QTM methods of measuring thermal conductivity. *Geothermics*, vol. 16, p. 215-226.

Hobart, M.A., Anderson, R.N., Fujii, N. and Uyeda, S. (1983) Heat flow from hydrothermal mounds in two million year old crust of the Mariana Trough which exceeds 2W/m^2. *EOS Trans.*, vol. 64, p. 315.

Honza, E. and Tamaki, K. (1985) The Bonin Arc. In *The ocean basins and margins, vol. 7A*, edited by A.E.M. Nairn *et al.*, Plenum Press, New York, p. 459-502.

Hussong, D.M., Uyeda, S. *et al.* (1982) *Init. Repts. DSDP*, vol. 60, Washington D.C. (U.S. Govt. Printing Office), 929 p.

Ito, Y., Saito, T., Nagumo, M. and Baba, K.

(1975) Box probe method for rapid determination of thermal conductivity of rocks. *Chinetsu*, vol. 12, p. 35-44 (in Japanese with English abstract).

Karig, D.E. (1971) Structural history of the Mariana Island Arc system. *Geol. Soc. Amer. Bull.*, vol. 82, p. 323-344.

——— and Moore, G.F. (1975) Tectonic complexities in the Bonin Arc system. *Tectonophysics,* vol. 27, p. 97-118.

Leg 126 Scientific Drilling Party (1989) ODP Leg 126 drills the Izu-Bonin arc. *Geotimes*, vol. 34, p. 36-38.

Lonsdale, P. and Hawkins, J. (1985) Silicic volcanism at an off-axis geothermal field in the Mariana Trough back-arc basin. *Geol. Soc. Amer. Bull.*, vol. 96, p. 940-951.

Martinez, F. and Cochran, J.R. (1989) Geothermal measurements in the northern Red Sea : implications for lithospheric thermal structure and mode of extension during continental rifting. *Jour. Geophys. Res.*, vol. 94, p. 12,239-12,265.

Matsubara, Y. (1981) Heat flow measurements in the Bonin Arc area. *Geol. Surv. Japan Cruise Rept.*, no. 14, p. 130-136.

Matsubayashi, O. (1982) Reconnaissance measurements of heat flow in the Central Pacific. *Geol. Surv. Japan Cruise Rept.*, vol. 18, p. 90-94.

Mogi, A. (1968) The Izu Ridge. In *Fossa Magna*, edited by M. Hoshino, Geol. Soc. Japan, Tokyo, p. 217-221 (in Japanese).

Moore, W.S. and Stakes, D. (1990) Ages of barite-sulfide chimney from the Mariana Trough. *Earth Planet. Sci. Lett.*, vol. 100, p. 265-274.

Mrozowski, C.L. and Hayes, D.E. (1979) The evolution of the Parece Vela Basin, eastern Philippine Sea. *Earth Planet. Sci. Lett.*, vol. 46, p. 49-67.

Murakami, F. (1988) Structural framework of the Sumisu Rift, Izu-Ogasawara Arc. *Bull. Geol. Surv. Japan*, vol. 39, p. 1-21.

———, Yamazaki, T., Saito, E. and Yuasa, M. (1989) Rifting and spreading processes at the northern Mariana Trough. *EOS Trans.*, vol. 70, p. 1313.

Nishimura, A. and Murakami, F. (1988) Sedimentation of the Sumisu Rift, Izu-Ogasawara Arc. *Bull. Geol. Surv. Japan*, vol. 39, p. 39-61.

———, Yamazaki, T., Yuasa, M., Mita, N. and Nakao, S. (1988) Bottom sample and heat flow data of Sumisu and Torishima Rifts, Izu-Ogasawara Arc. In *Geological map of Sumisu and Torishima Rifts, Izu-Ogasawara Arc, 1 : 200,000*, Marine Geology Map Series 31, Geological Survey of Japan.

Noel, M. (1984) Origins and significance of nonlinear temperature profiles in deep-sea sediments. *Geophys. J. R. astr. Soc.*, vol. 76, p. 673-690.

Ratcliffe, E.H. (1960) The thermal conductivities of ocean sediments. *J. Geophys. Res.*, vol. 65, p. 1535-1541.

Sager, W.W. (1980) Mariana Arc structure inferred from gravity and seismic data. *J. Geophys. Res.*, vol. 85, p. 5382-5388.

Sass, J.H., Stone, C. and Munroe, R.J. (1984) Thermal conductivity determinations on solid rock - a comparison between a steady-state divided-bar apparatus and a commercial transient line-source device. *J. Volcanol. Geotherm. Res.*, vol. 20, p. 145-153.

Sclater, J.G., Ritter, U.G. and Dixon, F.S. (1972) Heat flow in the southwestern Pacific. *J. Geophys. Res.*, vol. 77, p. 5697-5704.

Taylor, B., Brown, G., Fryer, P., Gill, J.B., Hochstaedter, A.G., Hotta, H., Langmuir, C.H., Leinen, M., Nishimura, A. and Urabe, T. (1990) ALVIN-SeaBeam studies of the Sumisu Rift, Izu-Bonin arc. *Earth Planet. Sci. Lett.*, vol. 100, p. 127-147.

Urabe, T. and Kusakabe, M. (1990) Barite silica chimneys from the Sumisu Rift, Izu-Bonin Arc : possible analog to hematitic chert associated with Kuroko deposits. *Earth Planet Sic. Lett.*, vol. 100, p. 283-290.

Vacquier, V., Uyeda, S., Yasui, M., Sclater, J., Corry, C. and Watanabe, T. (1966) Studies of the thermal state of the earth, 19th paper, heat-flow measurements in the Northwestern Pacific. *Bull. Earthq. Res. Inst.*, vol. 44, p. 1519-1535.

Villinger, H. and Davis, E.E. (1987) A new reduction algorithm for marine heat flow measurements. *J. Geophys. Res.*, vol. 92,

p. 12846-12856.

Watanabe, T., Epp., D., Uyeda, S., Langseth, M. and Yasui, M. (1970) Heat flow in the Philippine Sea. *Tectonophysics*, vol. 10, p. 205-224.

Yamano, M. (1985) Heat flow measurement. *In* Kobayashi, K. (ed.), *Preliminary Report of the Hakuho Maru Cruise KH84-1*, Ocean Research Institute, University of Tokyo, p. 265-271.

Yamazaki, T. (1988) Heat flow in the Sumisu Rift, Izu-Ogasawara (Bonin) Arc. *Bull. Geol. Surv. Japan*, vol. 39, p. 63-70.

——— (1992) Northern Mariana Trough. *In* Maruyama, S. *et al.* (ed.), *Orogeny of Japan* (submitted).

———, Ishihara, T. and Murakami, F. (1991) Magnetic anomalies over the Izu-Ogasawara (Bonin) Arc, Mariana Arc and Mariana Trough. *Bull. Geol. Surv. Japan*, vol. 42, p. 655-686.

———, Murakami, F., Saito, E. and Yuasa, M. (1988) Opening of the northern Mariana Trough. In *Tectonics of Eastern Asia and Western Pacific Continental Margin (Abstracts of the papers of the 1988 DELP Tokyo International Symposium)*, p. 25-26.

Yuasa, M. (1985) Sofugan Tectonic Line, a new tectonic boundary separating northern and southern parts of the Ogasawara (Bonin) Arc, Northwest Pacific. In *Formation of active ocean margins*, edited by N. Nasu *et al*, TERRAPUB, Tokyo, p. 483-496.

——— (1991) The reason for the differences in geologic phenomena between northern and southern parts of the Izu-Ogasawara Arc. *J. Geography*, vol.100, p.458-463 (in Japanese with English abstract).

——— (1992) Origin of the along arc variations of geologic phenomena on the volcanic front, Izu-Ogasawara Arc. *Bull. Geol. Surv. Japan*, vol. 43, in press.

Appendix

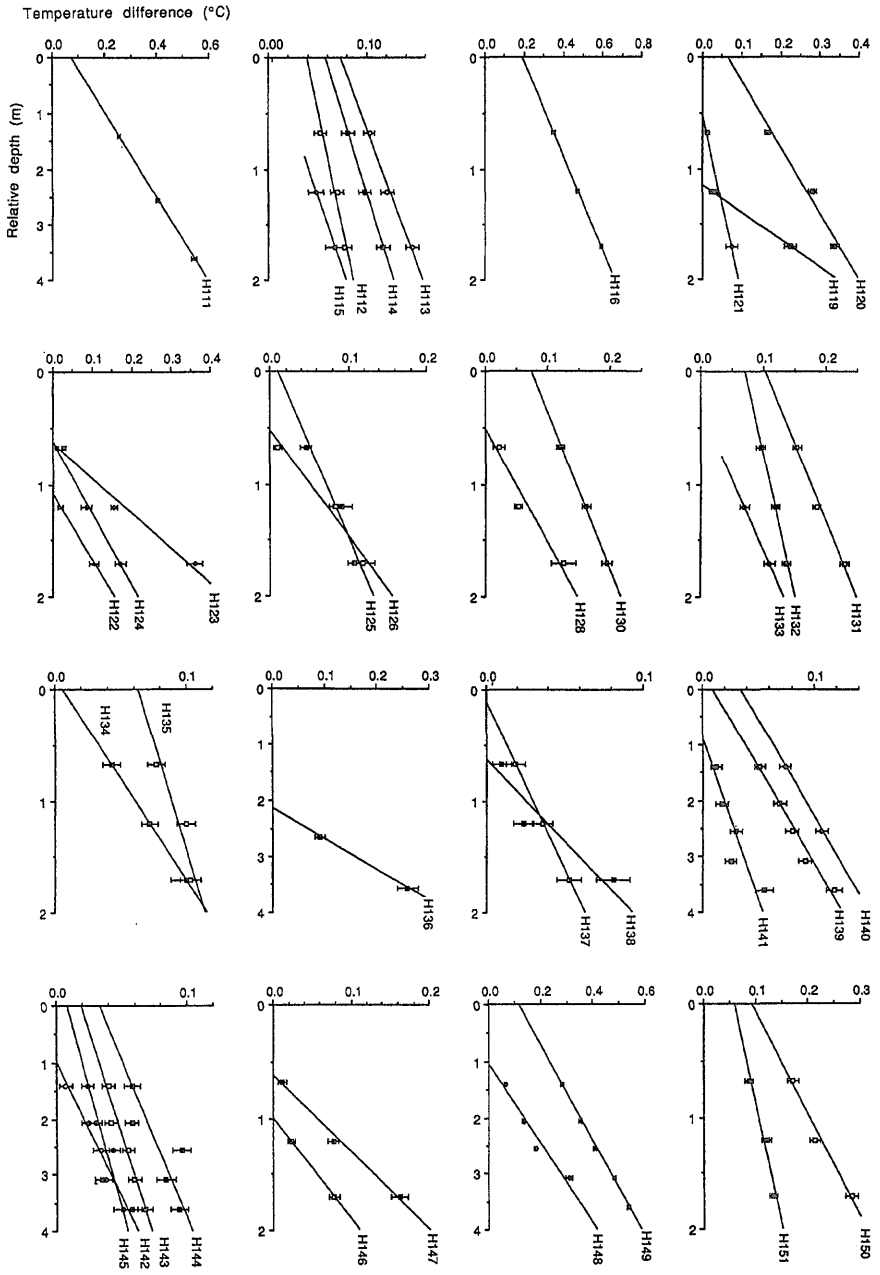

Fig. A-1 Sediment temperature profiles for all successful penetrations. Vertical axis represents the lengths of a probe. Horizontal axis represents difference from the temperature of bottom water just above the seafloor of each site. The uncertainty range is given for each temperature point according to the amount of frictional heating (see text). Thermal gradient is calculated by fitting a straight line using the least squares method if three or more temperature points are available. The points connected with dashed lines were not used for the calculation of the gradient (explained in the text).

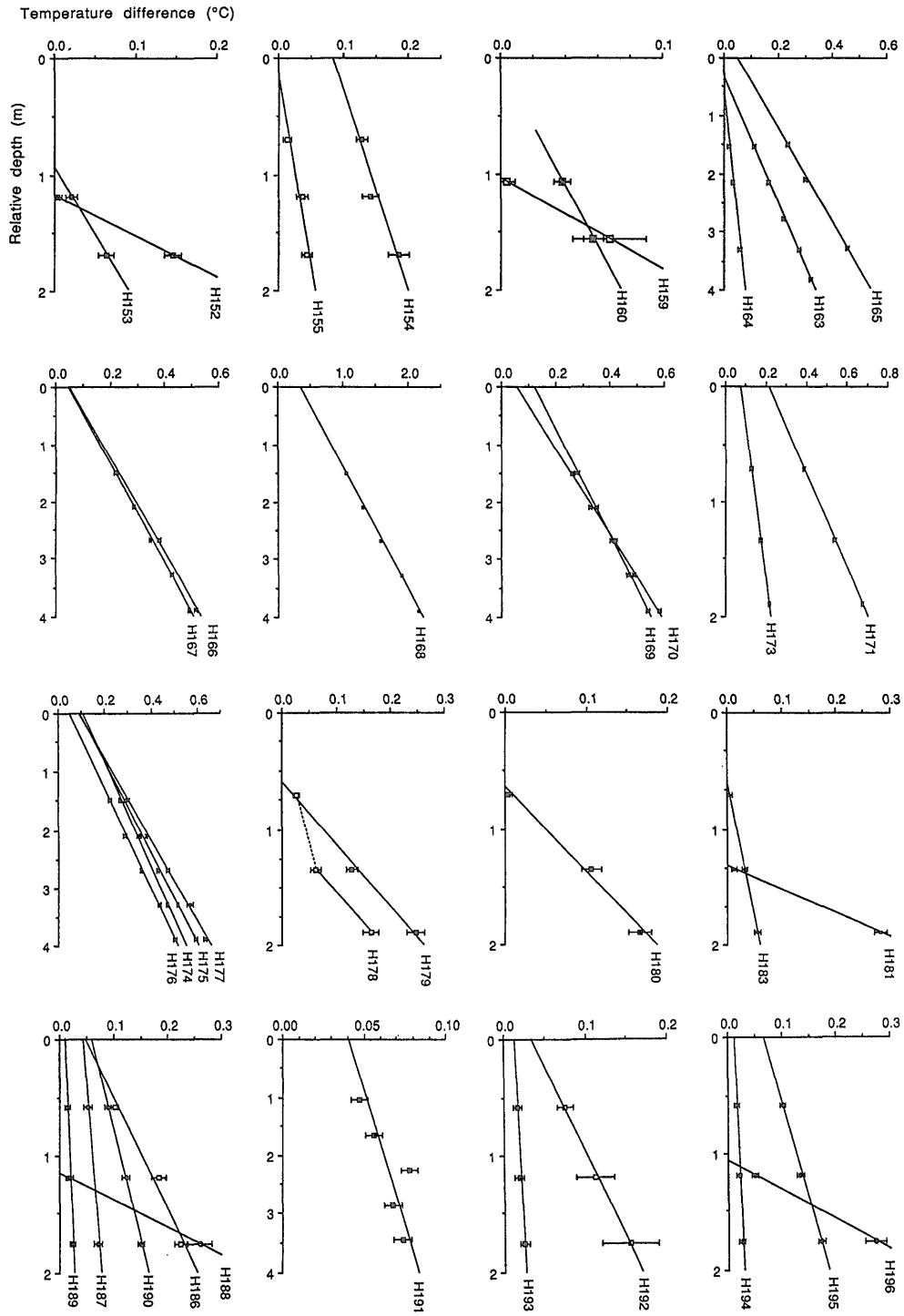

Fig. A-1 Continued

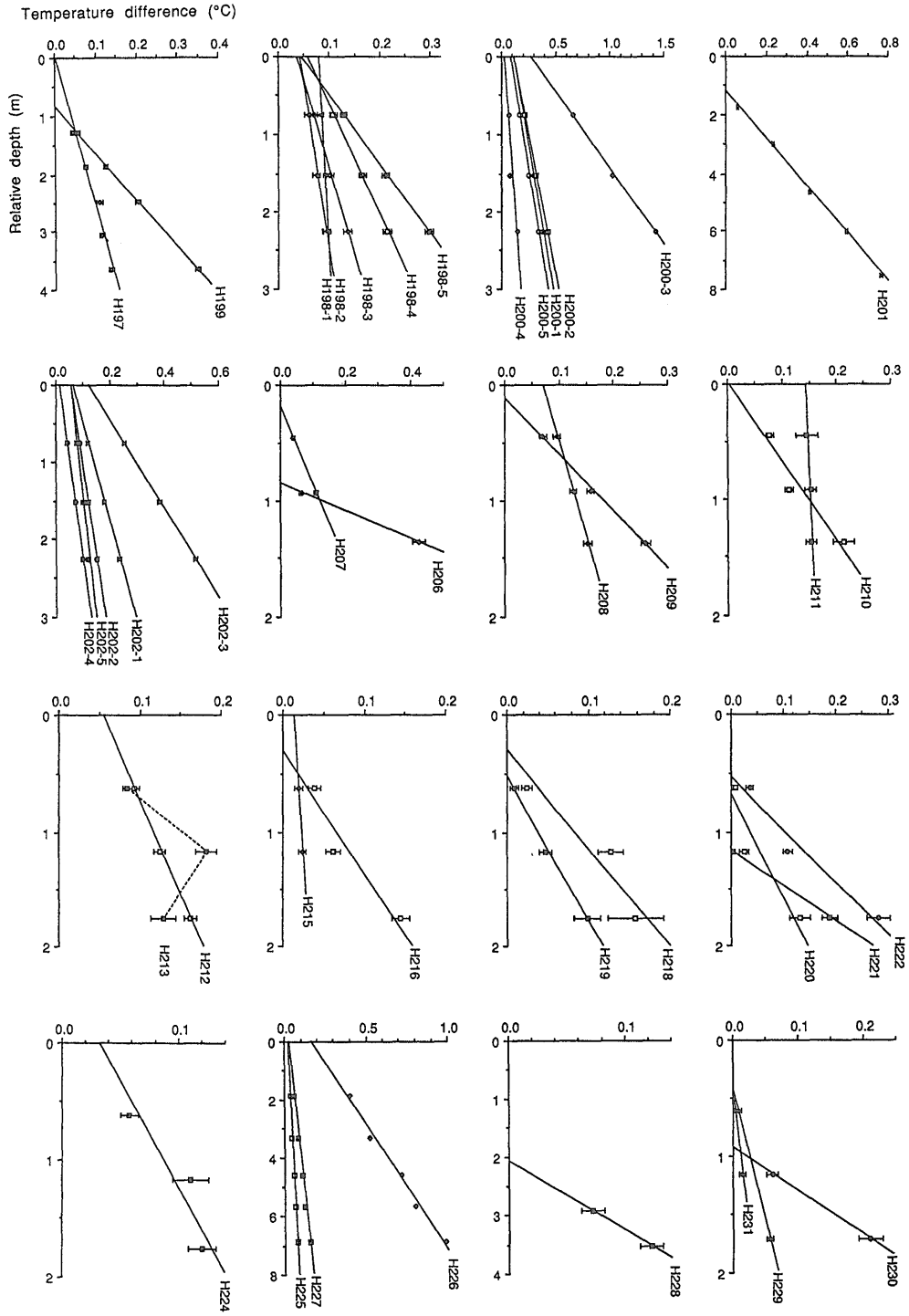

Fig. A-1 Continued

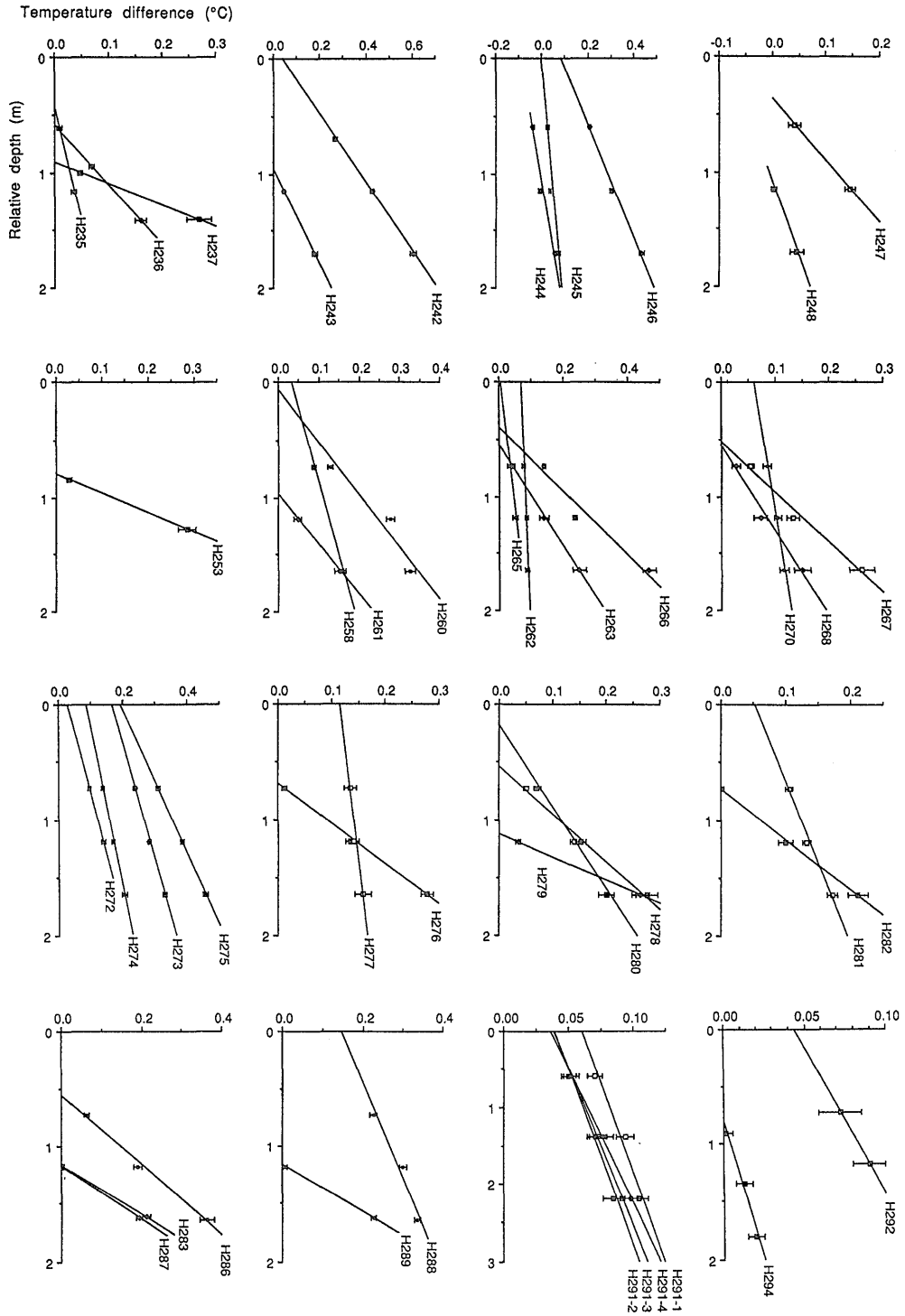

Fig. A-1 Continued

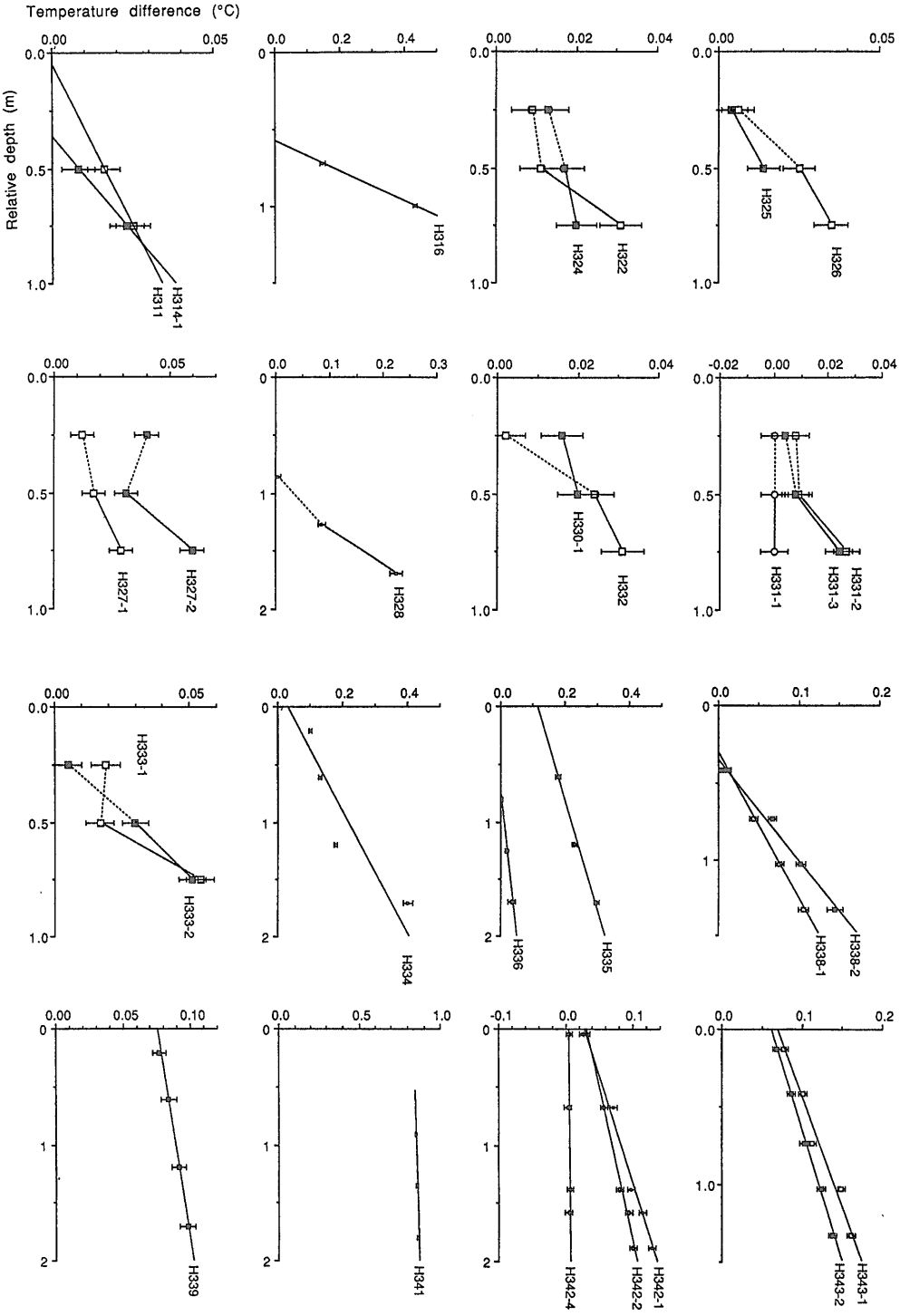

Fig. A-1 Continued

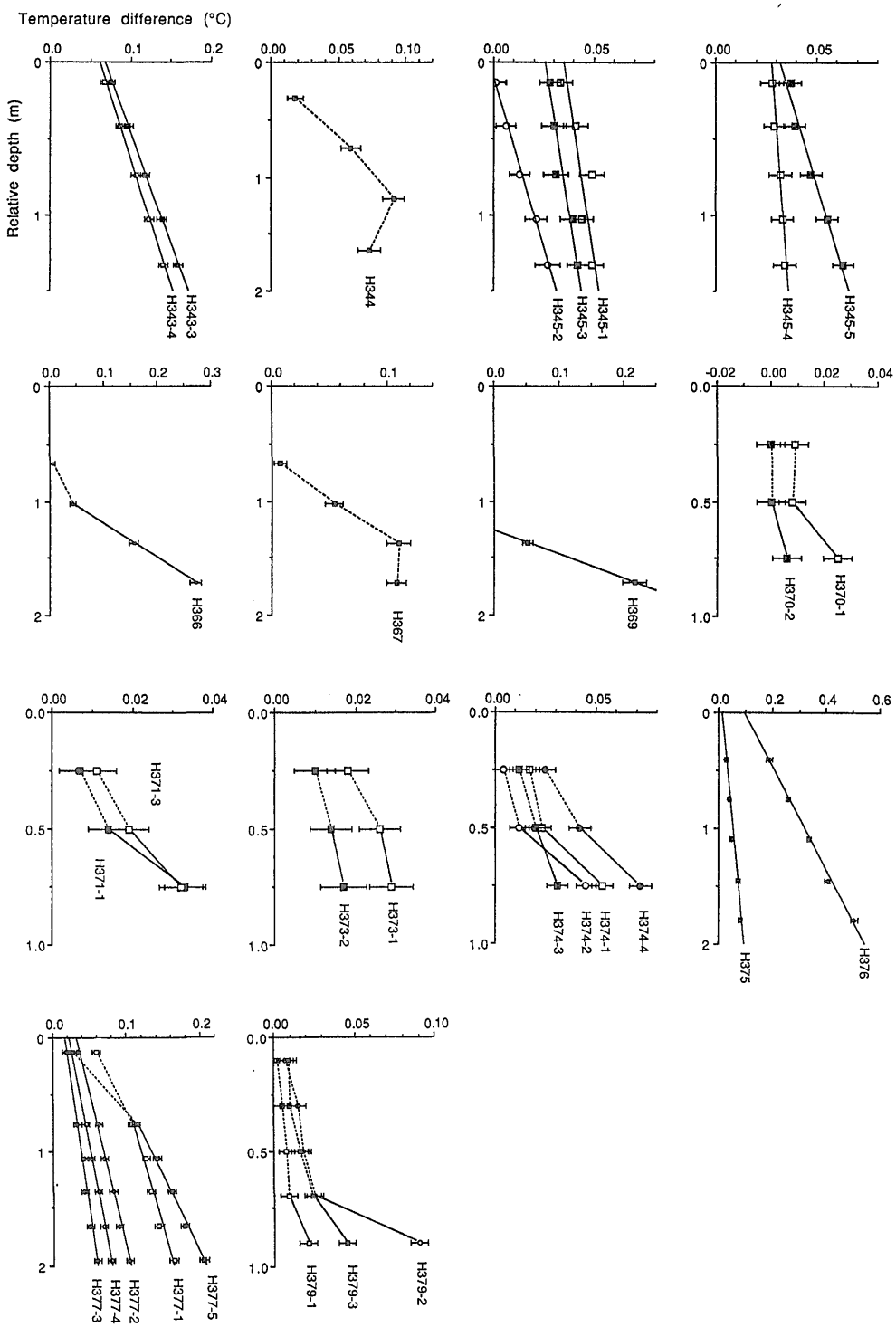

Fig. A-1 Continued

Table A-1 Summary of heat flow measurements.

Site No.	Lat.(N)	Lon.(E)	Depth	Probe	A	P	dT/dz	Ng	Cond.	s.d.	Nc	Q	Rem.	Area
H111 P442	30°51.75'	139°09.37'	2003	P4	2	F	0.131	3	0.981	0.035	15	129		
H112 RC350	30°03.92'	139°56.60'	2970	G2	1	F	0.023	3	0.862	0.032	9	20		Torishima Rift
H113 RC351	30°09.91'	139°40.26'	2207	G2	1	F	0.043	3	0.895	0.051	9	38	1	
H114 RC352	29°56.06'	139°38.58'	2550	G2	1	F	0.035	3	0.913	0.036	10	32		
H115 RC353	29°59.86'	140°01.91'	2975	G2	1	1.3	0.038	2	0.860	0.033	7	33	3	Torishima Rift
H116 RC354	29°55.98'	140°00.41'	2960	G2	2	F	0.237	3	0.864	0.031	10	205		Torishima Rift
H119 RC357	30°17.94'	139°57.70'	2480	G2	1	1.3	0.394	2	0.843	0.024	8	332	3	Torishima Rift
H120 RC358	30°13.92'	139°58.79'	2540	G2	2	F	0.167	3	0.866	0.036	10	145	2	Torishima Rift
H121 RC359	30°11.94'	140°01.40'	2538	G2	1	F	0.062	3	0.861	0.041	10	53		Torishima Rift
H122 RC360	29°39.95'	139°52.93'	2648	G2	1	1.3	0.167	2	0.854	0.028	8	142	3	Sofugan Is. -Nishinoshima Is.
H123 RC361	29°33.06'	140°12.79'	2649	G2	1	1.6	0.322	3	0.843	0.043	7	272	2	Sofugan Is. -Nishinoshima Is.
H124 RC362	29°26.88'	140°27.88'	2784	G2	1	1.6	0.156	3	0.867	0.016	7	135		Sofugan Is. -Nishinoshima Is.
H125 RC363	29°20.93'	140°35.31'	2808	G2	2	F	0.061	3	0.907	0.048	7	56		Sofugan Is. -Nishinoshima Is.
H126 RC364	29°17.98'	140°14.46'	3618	G2	1	1.6	0.106	3	0.868	0.026	8	92		Sofugan Is. -Nishinoshima Is.
H128 RC366	28°56.81'	140°39.29'	3651	G2	1	1.6	0.100	3	0.973	0.066	5	97		Sofugan Is. -Nishinoshima Is.
H130 RC368	28°39.07'	140°03.36'	2320	G2	1	F	0.072	3	0.933	0.010	8	67		Sofugan Is. -Nishinoshima Is.
H131 RC369	28°49.20'	140°03.23'	2719	G2	2	F	0.074	3	0.922	0.018	8	68		Sofugan Is. -Nishinoshima Is.
H132 RC370	28°50.73'	140°11.93'	2718	G2	1	F	0.040	3	0.958	0.028	8	38		Sofugan Is. -Nishinoshima Is.
H133 RC371	28°29.67'	140°35.26'	2653	G2	1	1.3	0.076	2	0.857	0.027	6	65	3	Sofugan Is. -Nishinoshima Is.
H134 RC372	28°14.93'	140°06.13'	2998	G2	1	F	0.055	3	0.876	0.029	9	48		Sofugan Is. -Nishinoshima Is.
H135 RC373	28°24.20'	140°04.95'	2644	G2	2	F	0.025	3	0.893	0.015	9	23		Sofugan Is. -Nishinoshima Is.
H136 P443	27°29.95'	141°18.23'	4123	P4	1	2	0.184	2	0.868	0.053	9	159	3	Ogasawara Trough
H137 RC374	29°14.84'	139°30.54'	3010	G2	1	F	0.033	3	0.935	0.021	8	31		
H138 RC375	28°59.97'	139°25.22'	3175	G2	1	F	0.069	3	0.905	0.037	9	62	2	
H139 P444	28°59.59'	139°50.02'	3038	P4	1+2	F	0.029	5	0.906	0.015	13	26		Sofugan Is. -Nishinoshima Is.
H140 P445	28°51.99'	139°47.84'	3303	P4	1+2	F	0.029	5	0.897	0.016	12	26		Sofugan Is. -Nishinoshima Is.
H141 P446	28°44.97'	139°47.04'	3531	P4	1+2	F	0.017	5	0.900	0.014	10	16		Sofugan Is. -Nishinoshima Is.
H142 P447	28°37.91'	139°36.95'	3638	P4	1+2	F	0.021	5	0.903	0.023	12	19		Sofugan Is. -Nishinoshima Is.
H143 P448	28°26.08'	139°35.78'	3485	P4	1+2	F	0.014	5	0.935	0.013	11	13		Sofugan Is. -Nishinoshima Is.
H144 P449	28°17.99'	139°33.90'	3550	P4	1+2	F	0.018	5	0.922	0.023	11	17		Sofugan Is. -Nishinoshima Is.
H145 P450	28°07.91'	139°30.94'	3597	P4	1+2	F	0.026	5	0.917	0.021	11	24		Sofugan Is. -Nishinoshima Is.
H146 RC376	27°59.63'	140°39.74'	3367	G2	1	1.3	0.110	2	0.913	0.065	9	100	3	Sofugan Is. -Nishinoshima Is.

Table A-1 Continued

H147 RC377	27°53.62'	140°40.27'	3574	G2	2	1.6	0.145	3	0.891	0.036	7	130		Sofugan Is. -Nishinoshima Is.
H148 P451	27°53.82'	140°09.06'	3715	P4	1+2	F	0.101	4	0.852	0.018	10	86	2	Nishinoshima Trough
H149 P452	27°45.09'	140°09.14'	3755	P4	1+2	F	0.118	5	0.828	0.030	11	98		Nishinoshima Trough
H150 RC378	27°44.96'	140°36.18'	3490	G2	2	F	0.110	3	0.902	0.057	9	100		Sofugan Is. -Nishinoshima Is.
H151 RC379	27°35.75'	140°32.15'	3585	G2	1	F	0.046	3	0.893	0.037	9	41		Sofugan Is. -Nishinoshima Is.
H152 RC380	31°16.95'	139°54.65'	1985	G2	1	1	0.284	2	[0.850]		0	241	3	Sumisu Rift
H153 RC381	31°07.67'	139°52.76'	2135	G2	1	1	0.086	2	0.840	0.024	6	72	3	Sumisu Rift
H154 RC382	26°59.97'	140°17.12'	3488	G2	1	F	0.059	3	0.885	0.025	9	52	1	Nishinoshima Trough
H155 RC383	26°58.32'	141°00.08'	2655	G2	1	F	0.031	3	0.880	0.031	8	28		North of Kaikata Smt.
H159 RC387	24°00.08'	141°33.02'	2253	G2	1	1	0.129	2	0.858	0.010	5	110	1,3	Mariana Trough
H160 RC388	24°02.68'	141°32.46'	2246	G2	1	1.3	0.039	2	0.823	0.033	5	32	1,3	Mariana Trough
H163 P453	27°20.02'	140°00.05'	3895	P4	1+2	F	0.093	5	0.849	0.025	9	79		Nishinoshima Trough
H164 P454	27°12.03'	140°00.09'	3778	P4	2	F	0.023	3	0.838	0.017	9	19		Nishinoshima Trough
H165 P455	27°00.06'	139°45.47'	3835	P4	1	F	0.124	3	0.829	0.028	11	103		Nishinoshima Trough
H166 P456	27°00.16'	139°47.55'	3845	P4	2	F	0.122	3	0.830	0.012	10	101		Nishinoshima Trough
H167 P457	27°00.10'	139°49.81'	3851	P4	1+2	F	0.115	5	0.823	0.023	9	95		Nishinoshima Trough
H168 P458	26°52.03'	139°45.85'	3845	P4	1+2	F	0.471	5	0.859	0.026	10	404		Nishinoshima Trough
H169 P459	26°52.00'	139°43.13'	3855	P4	1+2	F	0.107	5	0.825	0.040	10	88		Nishinoshima Trough
H170 P460	26°52.11'	139°44.85'	3851	P4	1+10	F	0.134	5	0.848	0.015	10	114		Nishinoshima Trough
H171 RC391	26°59.90'	139°43.75'	3802	G2	1	F	0.246	3	0.885	0.022	8	217		Nishinoshima Trough
H173 RC394	26°52.10'	139°39.46'	3845	G2	1	F	0.075	3	0.864	0.023	8	65		Nishinoshima Trough
H174 P461	26°50.62'	139°23.60'	4848	P4	1+10	F	0.111	5	0.789	0.018	10	88		Nishinoshima Trough
H175 P462	26°52.06'	139°46.66'	3835	P4	1+2	F	0.129	5	0.859	0.017	10	110		Nishinoshima Trough
H176 P463	26°52.15'	139°48.38'	3835	P4	2+10	F	0.118	5	0.839	0.032	10	99		Nishinoshima Trough
H177 P464	27°33.21'	139°59.87'	3795	P4	1+2	F	0.143	5	0.838	0.026	10	120		Nishinoshima Trough
H178 RC395	30°55.73'	139°41.23'	2220	G2	2	1.6	0.186	3	0.826	0.021	7	153	2	Sumisu Rift
H179 RC396	31°12.92'	139°54.63'	2123	G2	10	1.6	0.187	3	0.838	0.010	8	156		Sumisu Rift
H180 RC397	31°16.87'	139°53.99'	2045	G2	1	1.6	0.139	3	0.850	0.009	5	118		Sumisu Rift
H181 RC398	30°47.86'	139°53.56'	2293	G2	1	1	0.482	2	0.831	0.007	6	401	1,3	Sumisu Rift
H183 RC398	30°47.94'	139°42.72'	2235	G2	2	1.5	0.043	3	0.871	0.007	3	38		Sumisu Rift
H186 RC402	23°02.64'	142°04.42'	2560	G2	1	F	0.104	3	0.858	0.025	9	89		Mariana Trough
H187 RC403	22°56.12'	142°08.00'	3103	G2	2	F	0.017	3	0.805	0.051	8	14		Mariana Trough
H188 RC404	22°49.62'	142°34.66'	2928	G2	1	1	0.438	2	0.919	0.142	6	402	3	Mariana Trough
H189 RC405	22°36.84'	142°09.74'	3379	G2	1	F	0.009	3	0.766	0.034	8	7		Mariana Trough
H190 RC406	22°38.52'	142°18.16'	3471	G2	2	F	0.053	3	0.792	0.040	7	42	1	Mariana Trough
H191 P483	22°30.82'	142°18.95'	3483	P4	1+10	F	0.011	5	0.727	0.025	9	8		Mariana Trough

Table A-1 Continued

H192 RC407	22°33.99'	142°37.19'	3366	G2	1	F	0.068	3	0.970	0.113	8	66	1	Mariana Trough
H193 RC408	22°23.01'	142°17.40'	3385	G2	10	F	0.007	3	0.752	0.053	8	5		Mariana Trough
H194 RC409	21°51.14'	142°32.01'	4263	G2	1	F	0.009	3	0.739	0.012	8	6		Mariana Trough
H195 RC410	22°02.19'	142°39.06'	3884	G2	2	F	0.060	3	0.768	0.018	8	46		Mariana Trough
H196 RC411	22°12.33'	142°53.86'	4557	G2	10	1	0.396	2	0.841	0.003	3	333	3	Mariana Trough
H197 P484	27°06.18'	140°00.02'	3762	P4	1+2	F	0.039	5	0.856	0.033	9	33		Nishinoshima Trough
H198-1	27°07.63'	140°00.13'	3761	E2.5M	10	F	0.008	3	(0.856)		0	7		Nishinoshima Trough
H198-2	27°07.63'	140°00.13'	3760			F	0.024	3	(0.856)		0	21		Nishinoshima Trough
H198-3	27°07.45'	140°00.04'	3759			F	0.044	3	(0.856)		0	38		Nishinoshima Trough
H198-4	27°07.25'	139°59.92'	3760			F	0.071	3	(0.856)		0	61		Nishinoshima Trough
H198-5	27°07.14'	139°59.83'	3760			F	0.112	3	(0.856)		0	96		Nishinoshima Trough
H199 P485	26°49.96'	139°54.43'	3836	P4	1+2	F	0.124	4	0.840	0.027	9	104		Nishinoshima Trough
H200-1	26°52.26'	139°46.26'	3834	E2.5M	10	F	0.121	3	(0.859)		0	104		Nishinoshima Trough
H200-2	26°52.18'	139°46.14'	3836			F	0.138	3	(0.859)		0	119		Nishinoshima Trough
H200-3	26°52.00'	139°45.96'	3840			F	0.511	3	(0.859)		0	439		Nishinoshima Trough
H200-4	26°51.82'	139°45.82'	3841			F	0.052	3	(0.859)		0	45		Nishinoshima Trough
H200-5	26°51.70'	139°45.73'	3841			F	0.117	3	(0.859)		0	100		Nishinoshima Trough
H201 P486	27°05.33'	139°46.59'	3788	P8	1+2	F	0.124	5	0.849	0.017	15	105		Nishinoshima Trough
H202-1	27°07.33'	140°00.15'	3755	E2.5M	10	F	0.078	3	(0.856)		0	67		Nishinoshima Trough
H202-2	27°07.25'	140°00.10'	3757			F	0.043	3	(0.856)		0	37		Nishinoshima Trough
H202-3	27°07.17'	139°59.98'	3749			F	0.174	3	(0.856)		0	149		Nishinoshima Trough
H202-4	27°07.08'	139°59.81'	3760			F	0.039	3	(0.856)		0	34		Nishinoshima Trough
H202-5	27°06.93'	139°59.65'	3761			F	0.030	3	(0.856)		0	26		Nishinoshima Trough
H206	30°47.94'	139°54.03'	2290	E1.5	10	0.7	0.842	2	(0.831)		0	700	3	Sumisu Rift
H207	30°47.95'	139°54.32'	2288	E1.5	1	1.3	0.149	2	(0.831)		0	124	1,3	Sumisu Rift
H208	29°59.97'	140°01.56'	2980	E1.5	10	F	0.061	3	(0.874)		0	54		Torishima Rift
H209	29°59.80'	140°02.15'	2984	E1.5	1	F	0.204	3	(0.874)		0	179		Torishima Rift
H210	29°59.74'	140°02.38'	2970	E1.5	10	F	0.145	3	(0.874)		0	127	2	Torishima Rift
H211	29°59.88'	140°02.66'	2960	E1.5	1	F	0.008	3	(0.874)		0	7		Torishima Rift
H212 RC431	27°35.80'	140°32.92'	3567	G2	10	F	0.062	3	0.876	0.046	8	54		Sofugan Is. -Nishinoshima Is.
H213 RC432	27°53.90'	140°36.75'	3522	G2	10	F		3	0.910	0.055	7		4	Sofugan Is. -Nishinoshima Is.
H215 RC434	28°50.96'	140°35.15'	3765	G2	10	F	0.009	2	0.883	0.034	4	8	3	Sofugan Is. -Nishinoshima Is.
H216 RC435	28°49.29'	140°34.94'	3780	G2	1	F	0.094	3	0.919	0.050	3	87	1	Sofugan Is. -Nishinoshima Is.
H218 RC437	29°33.01'	140°05.31'	2913	G2	10	1.6	0.117	3	0.971	0.014	7	114	2	Sofugan Is. -Nishinoshima Is.
H219 RC438	29°32.99'	140°08.14'	2914	G2	1	1.5	0.083	3	0.941	0.093	7	78		Sofugan Is. -Nishinoshima Is.
H220 RC439	29°33.04'	140°10.69'	2812	G2	1	1.5	0.113	3	0.892	0.052	6	101	2	Sofugan Is. -Nishinoshima Is.

Table A-1 Continued

H221 RC440	29°32.97'	140°13.60'	2654	G2	10	1	0.340	2	0.854	0.008	4	290	3	Sofugan Is. -Nishinoshima Is.
H222 RC441	29°26.96'	140°32.06'	2840	G2	10	1.6	0.226	3	0.867	0.022	7	195	2	Sofugan Is. -Nishinoshima Is.
H224 RC443	27°30.10'	141°23.86'	4125	G2	10	F	0.057	3	0.870	0.026	5	50		Ogasawara Trough
H225 P488	24°48.77'	138°08.51'	5391	P8	1+10	F	0.008	5	0.785	0.027	14	6		Parece Vela Basin
H226 P489	24°26.99'	138°47.32'	5666	P8	2+10	F	0.117	5	0.764	0.024	12	90		Parece Vela Basin
H227 P490	24°44.70'	138°18.70'	5218	P8	1+10	F	0.019	5	0.795	0.035	15	15		Parece Vela Basin
H228 P491	24°43.53'	140°23.42'	3241	P4	1+10	1.5	0.085	2	(0.875)		0	74	1,3	West of Iwojima Is.
H229 RC444	24°41.12'	140°22.61'	3210	G2	1	1.5	0.044	2	(0.875)		0	38	3	West of Iwojima Is.
H230 RC445	24°28.05'	140°17.30'	3925	G2	10	1	0.271	2	0.875	0.019	3	237	1,3	West of Iwojima Is.
H231 RC446	24°29.27'	140°17.79'	3919	G2	10	1.5	0.020	2	(0.875)		0	17	3	West of Iwojima Is.
H235 RC450	29°59.96'	140°06.94'	2935	G2	1	1.5	0.051	2	(0.874)		0	44	3	Torishima Rift
H236	30°00.08'	140°05.55'	2931	E1.5	2	0.8	0.194	2	(0.874)		0	169	3	Torishima Rift
H237	29°59.83'	140°05.07'	2950	E1.5	1	0.8	0.539	2	(0.874)		0	471	1,3	Torishima Rift
H242 RC452	30°47.97'	139°53.13'	2270	G2	2	F	0.337	3	0.934	0.083	8	315		Sumisu Rift
H243 RC453	30°47.97'	139°52.44'	2260	G2	1	1	0.315	2	0.839	0.015	4	264	3	Sumisu Rift
H244 RC454	32°17.95'	139°42.51'	1579	G2	1	F	0.086	3	(0.930)		0	80	1,5	Aogashima Rift
H245 RC455	32°15.83'	139°47.78'	1595	G2	2	F	0.045	3	0.890	0.016	5	40	5	Aogashima Rift
H246 RC456	32°15.98'	139°45.24'	1609	G2	1	F	0.204	3	0.890	0.047	8	181	5	Aogashima Rift
H247 RC457	32°15.88'	139°39.82'	1589	G2	2	1.6	0.188	2	0.941	0.071	3	176	1,3,5	Aogashima Rift
H248 RC458	32°09.89'	139°39.95'	1610	G2	1	1	0.076	2	1.006	0.041	5	77	1,3,5	Aogashima Rift
H253	30°47.79'	139°55.63'	2280	G2	1	0.8	0.586	2	(0.830)		0	487	3	Sumisu Rift
H258 RC497	21°44.34'	143°52.21'	3544	G2	10	F	0.079	2	0.883	0.039	6	70	3	Mariana Trough
H260 RC499	21°36.62'	143°56.44'	3525	G2	2	F	0.220	3	0.877	0.027	7	193	2	Mariana Trough
H261 RC500	21°34.91'	143°57.18'	3512	G2	10	1	0.229	2	0.892	0.034	4	204	3	Mariana Trough
H262 RC501	21°27.12'	143°02.95'	4295	G2	10	F	0.012	3	0.786	0.037	8	10		Mariana Trough
H263 RC502	21°21.72'	143°15.36'	3917	G2	10	1.5	0.233	3	0.870	0.055	4	202		Mariana Trough
H265 RC504	22°53.76'	142°22.73'	3745	G2	10	F	0.040	2	0.981	0.118	6	39	3	Mariana Trough
H266 RC505	22°51.98'	142°24.23'	3745	G2	2	1.5	0.366	3	0.929	0.093	7	340	2	Mariana Trough
H267 RC506	22°49.57'	142°25.74'	3720	G2	10	1.5	0.232	3	0.989	0.085	7	230		Mariana Trough
H268 RC507	22°35.84'	142°36.31'	3375	G2	10	1.5	0.139	3	1.030	0.112	7	143		Mariana Trough
H270 RC509	22°28.25'	142°37.95'	3450	G2	2	F	0.036	3	0.970	0.099	8	35		Mariana Trough
H271 RC510	22°20.65'	142°34.01'	3375	G2	10	F	0.049	3	0.801	0.058	7	40		Mariana Trough
H272 RC511	22°34.82'	142°01.19'	2950	G2	10	F	0.096	2	0.795	0.021	8	76	3	Mariana Trough
H273 RC512	22°43.55'	142°03.71'	3140	G2	10	F	0.102	3	0.744	0.044	8	76		Mariana Trough
H274 RC513	22°44.39'	142°07.96'	3130	G2	2	F	0.074	3	0.793	0.027	8	59		Mariana Trough
H275 RC514	22°46.01'	142°16.02'	3450	G2	2	F	0.165	3	0.826	0.053	8	136		Mariana Trough

Table A-1 Continued

H276 RC515	22°46.95'	142°21.63'	3450	G2	10	1.4	0.299	3	0.871	0.056	6	260		Mariana Trough
H277 RC516	23°13.03'	142°08.56'	2730	G2	10	F	0.026	3	0.824	0.008	8	21		Mariana Trough
H278 RC517	23°15.02'	142°07.13'	2705	G2	2	1.5	0.252	3	0.817	0.006	6	205		Mariana Trough
H279 RC518	23°16.86'	142°04.10'	2710	G2	10	1	0.516	2	0.837	0.012	4	432	3	Mariana Trough
H280 RC519	23°13.56'	142°07.94'	2720	G2	2	F	0.145	3	0.805	0.012	7	117		Mariana Trough
H281 RC520	23°05.45'	142°02.48'	2530	G2	2	F	0.074	3	0.854	0.031	8	63		Mariana Trough
H282 RC521	23°11.57'	141°59.23'	2460	G2	10	1.3	0.238	3	0.809	0.013	5	193		Mariana Trough
H283 RC522	23°16.46'	142°03.16'	2710	G2	10	0.9	0.473	2	(0.830)		0	392	3	Mariana Trough
H286 RC525	23°15.48'	142°03.78'	2730	G2	10	1.5	0.334	3	0.825	0.011	7	276		Mariana Trough
H287 RC526	23°16.43'	142°02.19'	2685	G2	10	0.9	0.441	2	0.814	0.021	4	359	3	Mariana Trough
H288 RC527	26°41.31'	140°30.73'	3400	G2	10	F	0.121	3	0.864	0.034	7	105		West of Kaikata Smt.
H289 RC528	26°42.11'	141°19.84'	3280	G2	10	0.9	0.496	2	0.850	0.011	4	421	3	East of Kaikata Smt.
H291-1	28°37.78'	139°37.25'	3635	E2.5M	10	F	0.022	3	(0.920)		0	20		Sofugan Is. -Nishinoshima Is.
H291-2	28°37.79'	139°37.37'	3640			F	0.022	3	(0.920)		0	20		Sofugan Is. -Nishinoshima Is.
H291-3	28°37.91'	139°37.66'	3640			F	0.024	3	(0.920)		0	22		Sofugan Is. -Nishinoshima Is.
H291-4	28°38.07'	139°38.03'	3640			F	0.029	3	(0.920)		0	26		Sofugan Is. -Nishinoshima Is.
H292 RC530	27°30.08'	141°40.03'	4120	G2	10	F	0.039	3	0.851	0.028	6	33		Ogasawara Trough
H294 RC531	30°47.97'	139°55.11'	2285	G2	10	1.2	0.021	3	0.827	0.017	5	18		Sumisu Rift
H311	30°47.97'	139°54.90'	2285	B0.7	10	F	0.036	2	(0.830)		0	30	3	Sumisu Rift
H314-1	30°47.95'	139°55.95'	2280	B0.7M	10	F	0.060	2	(0.830)		0	50	3	Sumisu Rift
H316	26°41.60'	140°53.51'	1315	E1.0	10	0.5	1.063	2	(0.850)		0	904	3,5	Kaikata Smt.
H322	30°48.41'	139°53.53'	2290	B0.7	10	F	0.080	3	(0.830)		0	66		Sumisu Rift
H324	30°50.11'	139°53.09'	2285	B0.7	10	F	0.012	3	(0.830)		0	10		Sumisu Rift
H325	30°49.76'	139°53.17'	2285	B0.7	10	F	0.040	2	(0.830)		0	33	1,3	Sumisu Rift
H326	30°48.25'	139°53.46'	2290	B0.7	10	F	0.040	3	(0.830)		0	33		Sumisu Rift
H327-1	30°49.53'	139°53.22'	2290	B0.7M	10	F	0.048	3	(0.830)		0	40	1	Sumisu Rift
H327-2	30°49.34'	139°53.50'	2285			F	0.116	3	(0.830)		0	96	1,2	Sumisu Rift
H328 RC535	31°08.75'	139°56.22'	2045	G2	10	1.3	0.331	3	(0.850)		0	281		Sumisu Rift
H330-1	31°08.77'	139°56.30'	2050	B0.7M	10	F	0.016	2	(0.850)		0	14	3	Sumisu Rift
H331-1	30°48.10'	139°51.20'	2260	B0.7M	10	F	0.000	3	(0.830)		0	0		Sumisu Rift
H331-2	30°48.15'	139°51.71'	2260			F	0.072	3	(0.830)		0	60	1	Sumisu Rift
H331-3	30°48.22'	139°52.29'	2260			F	0.060	3	(0.830)		0	50		Sumisu Rift
H332	30°48.06'	139°50.82'	2240	B0.7	10	F	0.028	3	(0.830)		0	23		Sumisu Rift
H333-1	30°49.13'	139°53.19'	2290	B0.7M	10	F	0.148	3	(0.830)		0	123	1	Sumisu Rift
H333-2	30°48.95'	139°56.59'	2290			F	0.084	3	(0.830)		0	70	1,2	Sumisu Rift
H334 RC561	18°00.99'	144°53.31'	4405	G2	10+11	F	0.188	4	0.866	0.043	7	163	2	Mariana Trough

Table A-1 Continued

H335 RC562	18°00.84'	144°55.76'	3608	G2	10	F	0.106	3	0.857	0.067	5	91		Mariana Trough
H336 RC563	18°00.95'	145°01.22'	3770	G2	11	1.2	0.038	3	(0.857)		0	32		Mariana Trough
H338-1	18°00.94'	144°56.57'	3710	E1.5M	11	1.2	0.105	4	(0.857)		0	90		Mariana Trough
H338-2	18°00.92'	144°56.34'	3708			1.2	0.152	4	(0.857)		0	131		Mariana Trough
H339 RC564	20°54.16'	143°12.38'	4220	G2	11	F	0.014	4	0.744	0.013	6	10		Mariana Trough
H341 RC566	21°05.94'	143°18.12'	4392	G2	11	F	0.018	3	0.743	0.012	5	13	6	Mariana Trough
H342-1	21°05.81'	143°18.19'	4390	E1.5M	11	F	0.054	5	(0.743)		0	40		Mariana Trough
H342-2	21°05.60'	143°18.19'	4400			F	0.038	5	(0.743)		0	28		Mariana Trough
H342-4	21°05.15'	143°18.13'	4439			F	0.001	4	(0.743)		0	1		Mariana Trough
H343-1	21°10.70'	143°11.13'	3730	E1.5M	11	F	0.071	5	(0.743)		0	53		Mariana Trough
H343-2	21°10.49'	143°11.14'	3730			F	0.059	5	(0.743)		0	44		Mariana Trough
H343-3	21°10.31'	143°11.13'	3720			F	0.070	5	(0.743)		0	52		Mariana Trough
H343-4	21°10.11'	143°11.09'	3728			F	0.061	5	(0.743)		0	45		Mariana Trough
H344 RC567	21°30.52'	143°13.55'	3670	G2	11	F		4	0.828	0.026	6		4	Mariana Trough
H345-1	21°27.10'	143°02.72'	4298	E1.5M	11	F	0.012	5	(0.786)		0	9		Mariana Trough
H345-2	21°27.09'	143°02.50'	4296			F	0.022	5	(0.786)		0	18		Mariana Trough
H345-3	21°27.13'	143°02.26'	4292			F	0.012	5	(0.786)		0	10		Mariana Trough
H345-4	21°27.13'	143°02.01'	4291			F	0.005	5	(0.786)		0	4		Mariana Trough
H345-5	21°27.13'	143°01.73'	4287			F	0.023	5	(0.786)		0	18		Mariana Trough
H366 RC569	21°23.69'	143°14.54'	3915	G2	11	1.4	0.261	4	0.798	0.011	2	208		Mariana Trough
H367 RC570	21°30.53'	143°13.71'	3668	G2	11	1.4		4	0.840	0.019	6		4	Mariana Trough
H369 RC571	30°54.93'	139°51.28'	2245	G2	11	0.9	0.474	2	0.838	0.028	5	397	3	Sumisu Rift
H370-1	30°54.87'	139°51.75'	2275	B0.7M	10	F	0.068	3	(0.838)		0	56		Sumisu Rift
H370-2	30°54.80'	139°52.23'	2280			F	0.028	3	(0.838)		0	23		Sumisu Rift
H371-1	30°47.83'	139°53.60'	2290	B0.7M	10	F	0.072	3	(0.830)		0	60		Sumisu Rift
H371-3	30°47.82'	139°53.52'	2290			F	0.052	3	(0.830)		0	43		Sumisu Rift
H373-1	30°54.83'	139°53.41'	2280	B0.7M	10	F	0.012	3	(0.838)		0	10		Sumisu Rift
H373-2	30°54.75'	139°53.79'	2285			F	0.012	3	(0.838)		0	10		Sumisu Rift
H374-1	30°47.86'	139°53.93'	2280	B0.7M	10	F	0.120	3	(0.830)		0	100	2	Sumisu Rift
H374-2	30°47.65'	139°53.78'	2285			F	0.132	3	(0.830)		0	110	2	Sumisu Rift
H374-3	30°47.55'	139°53.51'	2285			F	0.044	3	(0.830)		0	37		Sumisu Rift
H374-4	30°47.46'	139°53.22'	2270			F	0.120	3	(0.830)		0	100		Sumisu Rift
H375 RC601	20°49.57'	144°38.40'	2555	G2	11	F	0.040	5	0.832	0.059	6	33		Mariana Trough
H376 RC602	20°49.02'	144°36.09'	2515	G2	11	F	0.224	5	0.852	0.065	7	191		Mariana Trough
H377-1	21°06.10'	143°17.90'	4405	E1.5M	11	F	0.043	6	(0.743)		0	40	6	Mariana Trough
H377-2	21°06.10'	143°17.69'	4352			F	0.037	6	(0.743)		0	27		Mariana Trough

Table A-1 Continued

H377-3	21°06.16'	143°17.54'	4352			F	0.022	6	(0.743)	0	16		Mariana Trough
H377-4	21°06.21'	143°17.28'	4345			F	0.029	6	(0.743)	0	22		Mariana Trough
H377-5	21°06.21'	143°17.04'	4300			F	0.075	6	(0.743)	0	56	6	Mariana Trough
H379-1	30°47.81'	139°53.82'	2295	B0.9M	11	F	0.060	5	(0.826)	0	50		Sumisu Rift
H379-2	30°47.90'	139°53.98'	2290			F	0.325	5	(0.826)	0	270	2	Sumisu Rift
H379-3	30°47.84'	139°54.19'	2290			F	0.105	5	(0.826)	0	87	2	Sumisu Rift

Foot note of Table

Probe : the type of thermistor probe used. G : a gravity corer with three to six thermistors in outrigger fashion (a number attached to the letter is the length of the probe), P : a piston corer with three to five thermistors in outrigger fashion, E : a lance without coring with three to six thermistors in outrigger fashion, B : a thin (20mm ϕ) Bullard type probe with three to five thermistors, M : multi-penetration measurement.

A : the apparatus used ; 1 : GH80-1-No.1, 2 : GH80-1-No.2, 10 : NTS10, 11 : NTS11

P : estimated penetration depth (m) ; F : full (or over) penetration.

dT/dz : thermal gradient (°K/m).

Ng : number of active thermistors in sediments.

Cond. : thermal conductivity (W/mK).

s.d. : standard deviation of the thermal conductivity data.

Nc : number of thermal conductivity measurements.

Q : heat flow (mW/m^2).

Remarks :

1. Accuracy of temperature data is low.
2. Non-linear temperature profile.
3. Gradient was calculated from only two temperature data.
4. Anomalous temperature profile.
5. Gradient may be affected by bottom water temperature variation because of shallow water depth.
6. Large temperature increase at very surface sediments.

伊豆・小笠原弧及びマリアナ弧の地殻熱流量

山 崎 俊 嗣

要 旨

伊豆・小笠原弧及びマリアナ弧において，1984年から1989年にかけて218点で新たに測定された熱流量値とその解釈を報告する．測定の目的は，熱水活動の可能性を評価することと，表記の海域のテクトニクスの理解を深めることであった．主に研究対象とした海域は，（1）伊豆・小笠原弧北部に発達する活動的背弧リフト群のひとつであるスミスリフト，（2）伊豆・小笠原弧中部に現在の島弧に斜交して存在する，漸新世の古リフトと考えられる西之島トラフの周辺，（3）北部マリアナトラフ（20°N-24°N）である．

スミスリフトでは高い熱流量を示す地点の存在及び分散の大きな熱流量分布より，熱水循環系の存在が推定される．ここでは，表層数十cmの温度勾配が異常に小さいことが多いが，底生生物の活動が盛んなことによる堆積物の擾乱が原因かもしれない．西之島トラフは，西側を正断層の急崖（孀婦岩構造線）により限られているが，熱流量はここを境にトラフ内では比較的高く，構造線の西側では低くなっている．このコントラストは，過去のリフティングに起因する地殻の厚さの差を反映しているものと推定される．西之島トラフ内には，貫入岩体に伴って局地的な高熱流量域が存在する．マリアナトラフの22°N 以北では現在リフティングが起こっているが，ここは熱的に非対称である．高熱流量はトラフの東縁のみで観測される．マリアナトラフの22°N 以南では，海洋底拡大が起こっており，拡大軸付近では熱水循環に起因すると考えられる異常な温度プロファイルが観測される．

（受付：1991年6月18日；受理：1991年7月24日）